

# Nanoscale

Accepted Manuscript



This is an *Accepted Manuscript*, which has been through the Royal Society of Chemistry peer review process and has been accepted for publication.

*Accepted Manuscripts* are published online shortly after acceptance, before technical editing, formatting and proof reading. Using this free service, authors can make their results available to the community, in citable form, before we publish the edited article. We will replace this *Accepted Manuscript* with the edited and formatted *Advance Article* as soon as it is available.

You can find more information about *Accepted Manuscripts* in the [Information for Authors](#).

Please note that technical editing may introduce minor changes to the text and/or graphics, which may alter content. The journal's standard [Terms & Conditions](#) and the [Ethical guidelines](#) still apply. In no event shall the Royal Society of Chemistry be held responsible for any errors or omissions in this *Accepted Manuscript* or any consequences arising from the use of any information it contains.

# Southwest University

College of Pharmaceutical Sciences, Chongqing 400716, P R China

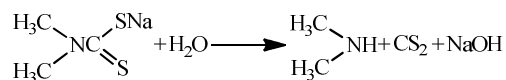
## Reponses to Reviewer 2

Dear Sir/Madam,

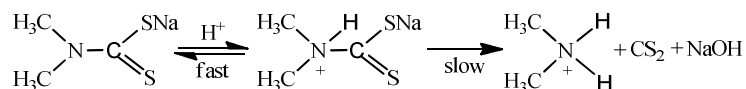
Thank you for your comments and suggestions on my manuscript that was submitted for publication in *Nanoscale* (Manuscript ID NR-ART-08-2015-005838.R1), and we benefit a lot. We have taken your comments seriously, and all revisions are highlighted with underscored red line in the main text. Following are detailed point-to-point responses to your comments:

[1] The authors claim the reactions of NaDDC degradation in neutral and alkaline conditions are the same because there are "OH" groups. In neutral conditions, there will be equal amount of "H<sup>+</sup>" in solution. Why the reaction would not be the same as the one in acidic conditions? Please explain.

**Response:** Thank you for your kind suggestion. The reaction is not the same in acidic conditions because the reaction mechanisms are different in this case. In acidic condition, the amine and alkali will be neutralized after the degradation of NaDDC (*Can. J. Bot.*, 1952, **30**, 131-138):



This can be accounted for by the following mechanism:



Research showed the kinetic data are in agreement with decomposition *via* a fast proton pre-equilibration step followed by subsequent decomposition of the protonated

## Southwest University

College of Pharmaceutical Sciences, Chongqing 400716, P R China

species to give the protonated amine and carbon disulphide (*Talanta*, 1969, **16**, 1099-1102).

However, in neutral conditions, there are much less  $H^+$  ions, so the protonation of amine can't occur, and thus the acidic decomposition of NaDDC. In neutral condition, there will be equal amount of  $H^+$  and  $OH^-$  in solution, but we use chemical formula the same with alkaline condition rather than acidic condition to describe the decomposition reaction in neutral condition for the following reasons:

1. NaDDC is easy to decompose in acidic condition (*Can. J. Bot.*, 1952, **30**, 131-138), but it is very stable in neutral and alkaline conditions (*Anal. Chem.*, 1970, **42**, 647-651). That is to say, in neutral condition, the acidic decomposition of NaDDC can't happen, so if NaDDC decomposes in neutral condition (with additional conditions to make the reaction easy to happen), it can only decompose in the way similar to the decomposition in alkaline condition.

2. In our research, AgNPs is the main driving force because it can form  $Ag_2S$  with  $S^{2-}$  released from NaDDC. Only in the basic decomposition of NaDDC, there is  $S^{2-}$  released (in acidic condition, NaDDC produces  $CS_2$  which could cause little change to the scattering light of AgNPs due to its much weaker rate of the sulfidation of Ag than  $S^{2-}$  (*Sci. Rep.*, 2015, **5**, 15427-15427)), so the decompositions in neutral and alkaline conditions are of the same kind.

3. In neutral condition, the experiment phenomenon is very similar to it in alkaline condition, and the reaction is milder. Considering that  $OH^-$  was the major reactant in the decomposition reaction of NaDDC and there are less  $OH^-$  ions in neutral condition than alkaline condition, combined with the fact that the decomposition of NaDDC in neutral condition is milder than it in alkaline condition, we can ascertain that the

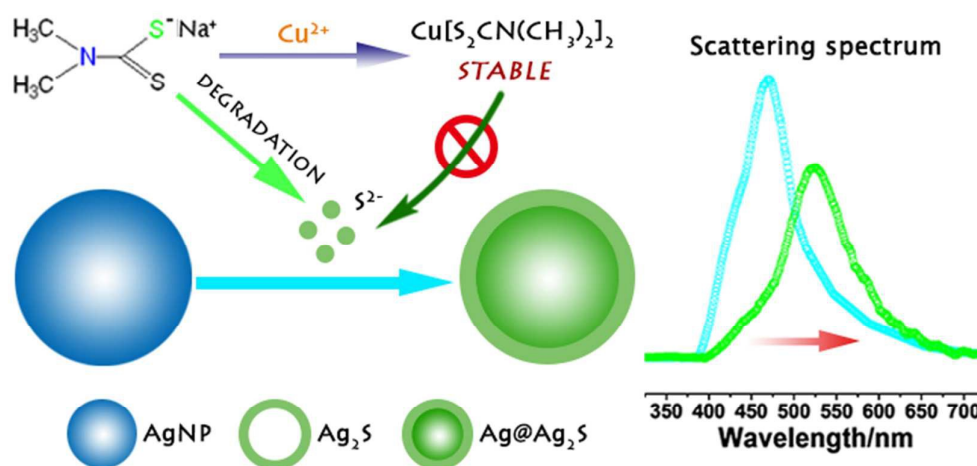
## Southwest University

College of Pharmaceutical Sciences, Chongqing 400716, P R China

decomposition mechanisms in neutral condition are the same with it in alkaline condition rather than acidic condition.

[2] The authors said the shoulder in the spectra in Figure 7A is due to error of the spectrograph device. If that is true, why no shoulder is observed in 7B and 7C? I don't think the error of the device is the cause of the shoulder. Is it possible from the irregular shape of the nanoparticles? Or "image charge" effect? Or coupling with nearby particles?

**Response:** We are very sorry for the mistake which could be avoided, and we have scanned the scattering spectrum in that condition again and redrawn the [Scheme 1](#). The spectrum chart in Scheme 1 is machined from previous experimental data to make it beautiful (without shoulder) and intuitive to show the spectrum change of the chosen AgNP before and after reaction.



The shoulder in Figure 7A is mainly due to error of the spectrograph device because of the following reasons:

1. The AgNP scattered blue light, so it was sphere rather than other shapes according to the previous report (*Nanoscale*, 2013, **5**, 7458-7466), thus excluding the

## *Southwest University*

College of Pharmaceutical Sciences, Chongqing 400716, P R China

irregular shape of AgNP;

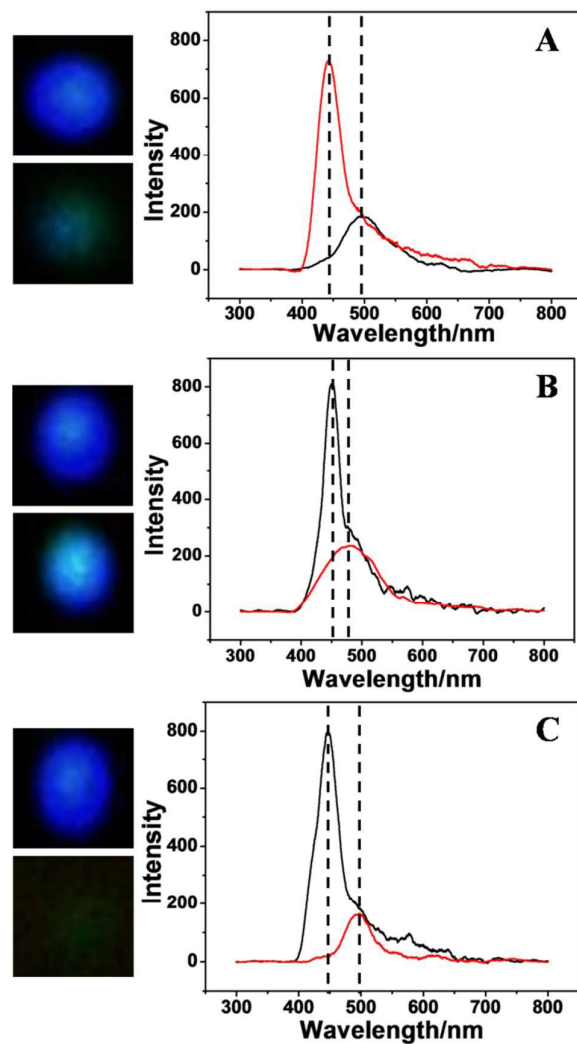
2. The chosen AgNP kept a farther distance with other AgNPs and it scattered blue light which was the characteristic scattering light color of single sphere AgNPs, so the cause of the shoulder shouldn't be coupling with nearby particles;

3. There is little consideration about the "image charge" effect of AgNPs in this research, but there are really some shoulders when using our spectrograph to scan single AgNPs for a while, and there is no shoulder observed for another while.

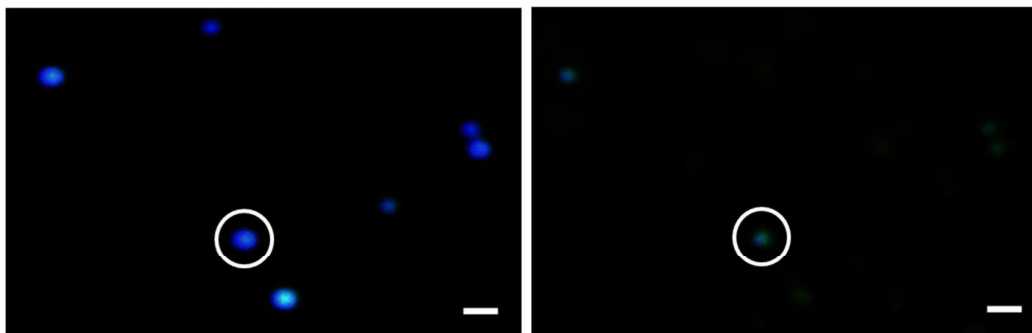
The shoulder may be also caused by the instability of AgNPs, because the impurities on the slide or O<sub>2</sub> in the water can both slightly influence the scattering light of AgNPs for its high reaction activity sometimes. When we scan the spectrum of single AuNPs, the shoulder seldom appears because AuNPs is more stable than AgNPs. We often repeat the experiment of scanning spectrum of single AgNPs before and after reaction many times to avoid this problem. Initially we thought the shoulder had little influence, but it indeed made the TOC unbeautiful and greatly reduced the quality of Figure 7A, so we repeated the experiment for Figure 7A (adding 1 mM NaDDC aqueous solution) several times, and finally obtained a good result (spectrum without shoulder). Figure 7 has been redrawn as following:

*Southwest University*

College of Pharmaceutical Sciences, Chongqing 400716, P R China



The following figure proves that the AgNP we scanned in Figure 7A is the same:



[3] The goal of the last part of the manuscript is not clearly defined. In the reply, the

## *Southwest University*

College of Pharmaceutical Sciences, Chongqing 400716, P R China

authors said their goal is to investigate the stoichiometric ratio between  $\text{Cu}^{2+}$  and NaDDC, which is already known, rather than test the stability of the complex. In that case, UV-vis of the supernatant can provide such information. Why did the authors choose to use DFM for such study? What is the advantage of DFM here?

**Response:** Thank you for your constructive suggestion. For its excellent ability of chelation with metal ions, NaDDC has been commercially used in metal finishing operations and treatment of wastewater by forming the metal precipitation. However, the disadvantages of NaDDC, such as uncontrollability of dosage, relatively high cost, difficulty in detecting the residual, potential liability for accident spills and overfeeding, have been found when used (*Met. Finish.*, 2001, **99**, 8-19). We have made detailed discussion about it in paragraph 4 in the INTRODUCTION. Applying our strategy with DFM can resolve these problems, because NaDDC could change the scattering light of AgNPs, if there is any NaDDC remaining in solution after chelation with metal ions, it can be detected through the change of scattering signals of AgNPs under DFM. The lowest response concentration of NaDDC is 10  $\mu\text{M}$ . Using DFM to investigate the stoichiometric ratio between  $\text{Cu}^{2+}$  and NaDDC can also make the result more intuitive and visualize the whole process. This is the advantage of DFM. We are sorry for the insufficient description of this issue and we have defined the goal of the last part clearly.

[4] Please remove "Finding out the mechanisms of the complex reaction could attribute to removing the hazards of NaDDC after degradation." I don't think the authors are trying to find the mechanism here.

**Response:** Thank you for your kind suggestion. We have removed the sentence, and

## *Southwest University*

College of Pharmaceutical Sciences, Chongqing 400716, P R China

have described the advantage of using DFM for investigation.

Your suggestions really help me a lot, and I am greatly appreciated for it again. If there is any question, please contact with me without hesitation.

Sincerely yours,

Cheng Zhi Huang, Ph. D. and Professor of Analytical Chemistry,

College of Pharmaceutical Sciences,

Southwest University,

Chongqing 400716, PRC.

E-mail: [chengzhi@swu.edu.cn](mailto:chengzhi@swu.edu.cn)

Tel: +86-23-68254659; Fax: +86-23-68367257

**Letter to Referees**

Chongqing, 2015-11-5

Dear Sir,

Thank you very much for your comments concerning our manuscript entitled “*Real-time scattered light dark-field microscopic imaging of the dynamic degradation process of sodium dimethyldithiocarbamate*” (Manuscript ID NR-ART-08-2015-005838R1). Your comments are well valuable and very helpful for revising and improving our paper, as well as important for guiding significance to our further researches.

Single nanoparticle analysis technique has caused wide attention with the aids of dark field microscopic imaging since it has high sensitivity. Considering that the long-term indiscriminate use of pesticides has led to the accumulation of them in the environments, forming harm to humans and causing secondary pollution after degradation, and investigations of the degradation process of pesticides can help understanding the degradation mechanisms and reducing the hazards of them, herein we made real-time monitoring of the decomposition dynamics of NaDDC in neutral and alkaline conditions by imaging single silver nanoparticles (AgNPs) under a dark-field microscopy (DFM) by taking sodium dimethyldithiocarbamate (NaDDC) as an example in this contribution.

I have tried our best to polish the manuscript, correct the errors in the manuscript carefully, and answer the reviewers’ questions, which we hope to meet with approval. The main corrections are highlighted with underscored red line in the paper and the responses to the reviewers’ comments have been attached.

I am greatly appreciated your work with our manuscript again, and if there is any question, please contact with me without hesitation.

Sincerely yours,

Cheng Zhi Huang, Ph. D. and Professor of Analytical Chemistry,  
College of Pharmaceutical Sciences, Southwest University,  
Chongqing 400716, PRC.

E-mail: [chengzhi@swu.edu.cn](mailto:chengzhi@swu.edu.cn)

Tel: +86-23-68254659; Fax: +86-23-68367257



Journal Name

ARTICLE

# Real-time scattered light dark-field microscopic imaging of the dynamic degradation process of sodium dimethyldithiocarbamate

Gang Lei,<sup>a</sup> Peng Fei Gao,<sup>a</sup> Hui Liu\*<sup>a</sup>, and Cheng Zhi Huang\*<sup>a,b</sup>Received 00th January 20xx,  
Accepted 00th January 20xx

DOI: 10.1039/x0xx00000x

[www.rsc.org/](http://www.rsc.org/)

Single nanoparticle analysis (SNA) technique has caused wide attention with the aid of dark-field microscopic imaging (iDFM) technique owing to its high sensitivity. Considering that the degradation of pesticides can bring about serious problems in food and environment and real-time monitoring the dynamic degradation process of pesticides can help understanding and defining their degradation mechanisms, herein we made real-time monitoring of the decomposition dynamics of sodium dimethyldithiocarbamate (NaDDC) in neutral and alkaline conditions by imaging single silver nanoparticles (AgNPs) under a dark-field microscope (DFM) by taking this pesticide as an example, in which the localized surface plasmon resonance (LSPR) scattering signals were measured at single nanoparticle level. As a result, the chemical mechanism of the degradation of NaDDC in neutral and alkaline conditions was proposed, and the inhibit effects of metal ions including Zn (II) and Cu (II) were investigated in order to understand the decomposition process in environments. It was found that Cu (II) can form a most stable complex with NaDDC with a stoichiometric ratio of 2:1, greatly reduces the toxicity.

## Introduction

Single nanoparticle analysis (SNA) technique, developed by using the localized surface plasmon resonance (LSPR) scattering signals of single noble metal nanoparticles by dark-field microscopic imaging (iDFM), has attracted much attention and has been widely employed in biosensing, chemical detection and cellular imaging in recent years.<sup>1-4</sup> SNA technique is more accurate than conventional analytical methods because every single nanoparticle can serve as an independent sensor in iDFM.<sup>5</sup> For example, resonance light scattering technique in solution has been widely applied for analytical purposes, wherein the signals measured for analysis were obtained from an ensemble of nanoparticles or aggregates.<sup>6,7</sup> We noticed that one of the important research fields of SNA technique is to be applied for the real-time monitoring of chemical reactions, including organic reactions, nanoalloy-growth, cellular processes and so on.<sup>8-11</sup> However, investigations for the degradation process of pesticides, which can help understanding and defining their degradation mechanisms, are not involved up to now.

It is known that the long-term indiscriminate use of pesticides has led to the accumulation of them and brought about serious problems in food and environment.<sup>12</sup> In fact, less than 0.3% of the pesticides applied actually reaches their targeted pests,<sup>13</sup> and thus about 99.7% of the remaining forms are harmful to the non-target organisms and causes secondary pollution after degradation. There have been various stakeholders to reduce or eliminate the use of pesticides, but the degradation mechanisms possessing crucial significance in decreasing their side effects remain unclear and challengeable.<sup>14,15</sup>

Monitoring the degradation process of pesticides by using iDFM technique to monitor the LSPR optical properties of AgNPs was a feasible alternative, since iDFM technique takes advantages of high efficiency, less time consuming and high signal-to-noise ratio by investigating the shape, size, composition and surrounding medium of nanoparticles.<sup>16-18</sup> Although there are many researches using AgNPs as a chemical probe,<sup>19-21</sup> the application of iDFM technique to monitor the degradation process of pesticides through observation of the dynamic changes in LSPR scattered light of single AgNPs has not been developed up to now.

Sodium dimethyldithiocarbamate (NaDDC), a common pesticide,<sup>22</sup> is also a kind of dithiocarbamate acids (DTC). Most of the investigations about the decomposition mechanisms of NaDDC are conducted through measuring the amount of CS<sub>2</sub> under acidic condition,<sup>23-25</sup> but the decomposition mechanisms of NaDDC in neutral and basic conditions have been neglected for a long time due to the fact that the dialkyl DTC are very stable in these conditions.<sup>26</sup> It was reported that after reacting with the corresponding chlorides,

<sup>a</sup> Key Laboratory of Luminescent and Real-Time Analytical Chemistry (Southwest University), Ministry of Education, College of Pharmaceutical Sciences, Southwest University, Chongqing 400716, P. R. China. Fax: +86 23 68367257; Tel: +86 23 68254059. E-mail: liuhui78@swu.edu.cn

<sup>b</sup> Chongqing Key Laboratory of Biomedical Analysis (Southwest University), Chongqing Science & Technology Commission, College of Chemistry and Chemical Engineering, Southwest University, Chongqing 400715, China. Fax: +86 23 68367257; Tel: +86 23 68254659. E-mail: chengzhi@swu.edu.cn

† Electronic Supplementary Information (ESI) available: [additional DFM images (Fig.S1-S9) and the typical dynamic iDFM of monitoring (Movie S1-S2)]. See DOI: 10.1039/b000000x/

the product of NaDDC can degrade into RSNa, Na<sub>2</sub>S, Na<sub>2</sub>CO<sub>3</sub> and NH(CH<sub>3</sub>)<sub>2</sub>, when heated under reflux for five hours with five moles of aqueous alcoholic alkali.<sup>27</sup> Nonetheless, the mechanisms of the basic decomposition of NaDDC are not clear until now. Therefore, NaDDC was selected as an example to investigate the degradation process of pesticides in this study.

Establishing a highly sensitive dynamic detection method and quantitatively real-time monitoring the decomposition process of NaDDC is of great environmental significance as well. NaDDC has various applications in agriculture, industry and medicine.<sup>22</sup> If uptaken by the plants, NaDDC would transformed into other fungitoxic compounds to achieve therapeutic effect.<sup>28</sup> For its excellent ability of chelation with metal ions, NaDDC has also been commercially used in metal finishing operations and treatment of wastewater by forming the metal precipitation.<sup>29, 30</sup> However, the disadvantages of NaDDC use, such as uncontrollability of dosage, relatively high cost, and difficulty in detecting the residual have been found.<sup>31</sup> Mover, NaDDC is considered as an important precursor of NDMA, a suspected carcinogen,<sup>32, 33</sup> and will produce toxic CS<sub>2</sub> after acidic decomposition.<sup>25</sup> Conventional techniques employed in the detection of NaDDC, such as UV absorption spectra,<sup>34</sup> high-performance liquid chromatography (HPLC),<sup>35</sup> and capillary electrophoresis,<sup>36</sup> suffer problems of high detection limits, complicated operations and inferior efficiency. In contrast, single nanoparticle analysis technique can be used as a new dominant platform for the detection of NaDDC or other pesticides.

By using iDFM at single nanoparticle level to quantitatively resolve the dynamic process in terms of mechanisms understanding of the reaction,<sup>37</sup> herein we monitor the decomposition reaction of NaDDC in both neutral and basic conditions on the basis of the reaction between the S<sup>2-</sup> which released from the degradation process and AgNPs which acts as a nanoprobe for it can result in decreasing LSPR light scattering signals.

## EXPERIMENTAL SECTION

### Materials

Sodium citrate (Na<sub>3</sub>C<sub>6</sub>H<sub>5</sub>O<sub>7</sub>·2H<sub>2</sub>O AR, 99.0%) and copper sulfate (CuSO<sub>4</sub>·5H<sub>2</sub>O AR, 99.0%) were obtained from Tianjin Regent Chemicals Co. Ltd.. Silver nitrate (AgNO<sub>3</sub> AR, 99.8%) was purchased from Shanghai Shenbo Chemical Engineering Co. Ltd.. Glycerin was obtained from Chongqing Chuandong Chemical (Group) Co. Ltd.. Zinc sulfate (ZnSO<sub>4</sub> AR, 99.5%) was purchased from Hunan Xiangzhong Geological Experiment Research Institute. Sodium Dimethyldithiocarbamate (C<sub>3</sub>H<sub>6</sub>NNaS<sub>2</sub>·2H<sub>2</sub>O AR, 98.0%) was acquired from Beijing J & K Technology Co. Ltd.. Other chemicals were analytical reagent grade and were used without further treatment. Milli-Q purified water (18.2 MΩ at 25 °C) was used throughout.

### Apparatus

Scattered light iDFM technique was carried out through a BX51 optical microscope (Olympus, Japan) equipped with a high numerical dark-field condenser (U-DCW, 1.2–1.4). The scattered light was collected by a 100× objective lens and the images were taken by a DP72 single chip true color CCD camera (Olympus,

Japan). The images were analyzed with Image-Pro Plus 6.0 (IPP) software (Media Cybernetics, USA). The size and morphology of the AgNPs were imaged by a Hitachi S-4800 scanning electron microscopy (SEM, Tokyo, Japan). The UV-vis absorption spectroscopy of NaDDC was performed with a UV-3600 spectrophotometer (Hitachi, Tokyo, Japan). A vortex mixer (QL-901, Kylin-Bell, Haimen, China) was used to blend the solutions. A centrifuge (H1650-W, Xiangyi, Hunan, China) was employed to separate the precipitates and supernatants.

### Preparation of AgNPs

AgNPs were prepared using previously reported methods. Firstly, a 50 mL glycerol/water mixture (20 vol% glycerol) was stirred (1200 rpm, 2.5 cm stirring bar) in a 100 mL flask and heated up to 95°C. Then, 9 mg silver nitrate was added to the solution, and 1 min later, 1 mL sodium citrate (3%) was added into the mixture again. The reaction mixture was stirred for 1 h at 95°C. The color change rate of the solution was found to be slightly slower than that of the classical Lee and Meisel method.<sup>38</sup> After the reaction completed, the colloid was stored at 4 °C.

### Scattered light iDFM of AgNPs

To observe the scattered light changes of AgNPs either in intensity or color during its reaction with NaDDC, a homemade device with of a slide glass and cover glass was used to produce a simulated flow cell.<sup>8</sup> Scattered light iDFM of AgNPs deposited at the bottom of the cell were taken and an area containing AgNPs was selected for real-time monitoring. The NaDDC solution was added into the cell to initiate the degradation in neutral and alkaline conditions, respectively. The phosphate buffer (PB) was used to create an alkaline environment of pH 9.0. Then, the scattered light iDFM of the same area were obtained at different time points.

### The inhibition of metal ions on the degradation of NaDDC

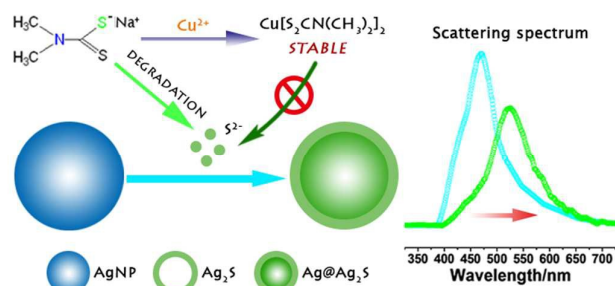
Like most pesticides, NaDDC would produce toxic substances after degradation. Besides decreasing the usage amount, inhibiting its degradation in the environment was also a way to reduce the environmental hazards of NaDDC. As mentioned before, metal ions could form complex with NaDDC, thus inhibiting its degradation, so we involved this facet of the research later. Herein Cu<sup>2+</sup> and Zn<sup>2+</sup> ions were chosen for the inhibition experiment. Particularly, the inhibition of Cu<sup>2+</sup> on the degradation of NaDDC was made in neutral and alkaline conditions because the complex of Cu<sup>2+</sup> and NaDDC was most stable.

### Data analysis

The statistics of light intensity and the red, green and blue (RGB) color proportion of the scattered light of AgNPs at single nanoparticle level were carried out using Image-Pro Plus (IPP) 6.0 software.<sup>16</sup>

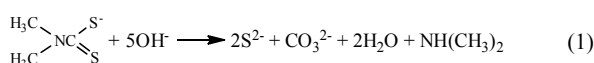
## RESULTS AND DISCUSSIONS

### Principle of the real-time imaging of the dynamic degradation of NaDDC.

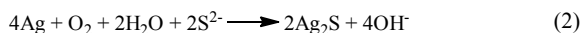


**Scheme 1.** Schematic illustration of real-time monitoring of the degradation process of NaDDC by using the LSPR scattering light of AgNPs and the inhibition of metal ions such as Cu (II) ions.

When decomposition of NaDDC occurred,  $S^{2-}$  might be released according to references:<sup>27</sup>



Nevertheless, the reaction is very difficult to happen at room temperature. In such case, the presence of Ag in neutral and alkaline conditions makes the chemical equilibrium of equation 1 constantly shift to right since the generated  $S^{2-}$  can form  $\text{Ag}_2\text{S}$  with it:<sup>39-41</sup>



which supplies the monitoring with an exciting way. That is to say, single AgNPs can act as a good nanoprobe to monitor the decomposition reaction of NaDDC in neutral and basic conditions (Scheme 1) since the LSPR optical properties of silver nanoparticles (AgNPs) are sensitive to their surrounding environments,<sup>42, 43</sup> and the changes in scattering intensity and color of AgNPs could be observed and be used as the detecting signals.<sup>44, 45</sup>

### Interaction between AgNPs and NaDDC

The as-prepared AgNPs had an average size of  $47.69 \pm 6.65$  nm, with a very narrow dispersion (Fig. 1A), displaying a yellow LSPR absorption band characteristic at 409.5 nm and blue scattering characteristic at 442 nm (Fig. 1B). The scattered blue light of the AgNPs ensemble in the solution was identical to those deposited on the glass slide under a white light source (Fig. S1†). Owing to the nonuniformity of AgNPs, there were some nanoparticles scattering other colors,<sup>46</sup> but we only considered the blue spherical particles.

The LSPR features either absorption or scattering are sensitive to the environments.<sup>47, 48</sup> Fig. 2A-F showed that the time-dependent

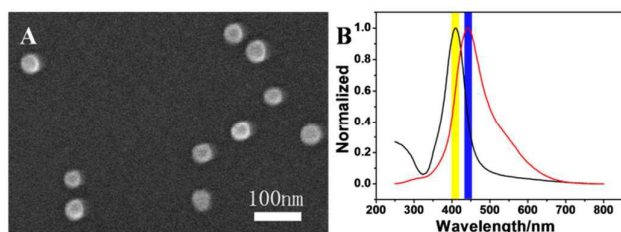


**Fig. 1** The characterization of the synthetic AgNPs: (A) SEM images and (B) UV absorption (black) and LSPR scattering (red) spectra.

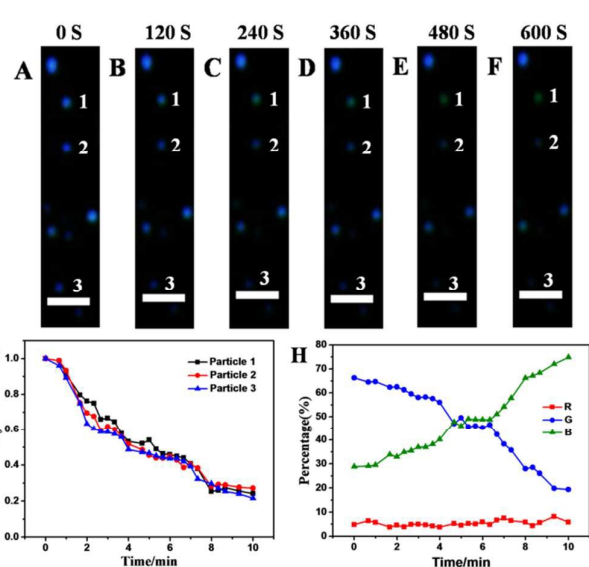


**Fig. 2** Scattered light iDFM of AgNPs during its reaction with NaDDC: (A-F) time-dependent images captured at different time points, with a latency time of 120s;  $\text{C}_{12}\text{H}_{18}\text{N}_4\text{S}_2$ ,  $1.0 \times 10^{-3}$  mol  $\text{L}^{-1}$ ; pH, 7; (G) time-dependent intensity analysis of the corresponding particles in (A-F); (H) time-dependent RGB analysis of the color-changed Particle 1 in (A-F). The scale bar is 2  $\mu\text{m}$  for all images.

evolution process of the scattered light iDFM for these AgNPs with the addition of 1 mM NaDDC aqueous solution. The blue scattering light of the AgNPs gradually declined with the addition of NaDDC, and some of the scattering light changed from blue to green (Particles 1 in Fig. 2A-F). This process remains about 10 min, and most of the blue spots disappeared. It should be noted that there were still some blue AgNPs on the glass (Particle 2 and 3) in which slight changes have occurred, displaying that the evolution process of different AgNPs are particle dependent in terms of the shape, the size and surficial state. The light intensity of three typical particles and the RGB proportion of the color-changed particle were analyzed to quantify the scattering light of AgNPs. As shown in Fig. 2G, the light intensity of Particles 1–3 gradually decreased to lower than 30% of their original light intensity. Moreover, the change of RGB proportion of Particle 1 which turned green after reaction was identical to the color changes that were observed by imaging (Fig. 2H). With the increase of reaction time, percentage of blue (PB) gradually decreased from 66% to 19%, while percentage of green (PG) gradually increased from 29% to 75%. Percentage of red (PR) was always maintained at 4–8% during the whole degradation process of NaDDC.

The evolution process of the scattered light iDFM for these AgNPs with the addition of NaDDC discloses the reaction features. The HRTEM images (Fig. 3A and B) showed that a very thin layer of  $\text{Ag}_2\text{S}$  has really formed on the surface of the AgNPs. The EDS analysis (Fig. 3C) evidenced the content of S was about 2%. Although the content was ultralow, it could lead to obvious variation in dark-field imaging.<sup>45</sup> That is to say,  $\text{Ag}_2\text{S}$  layer has been really formed, reflecting the release of  $S^{2-}$  in both in neutral and alkaline conditions, which is the main driving force of degradation reaction

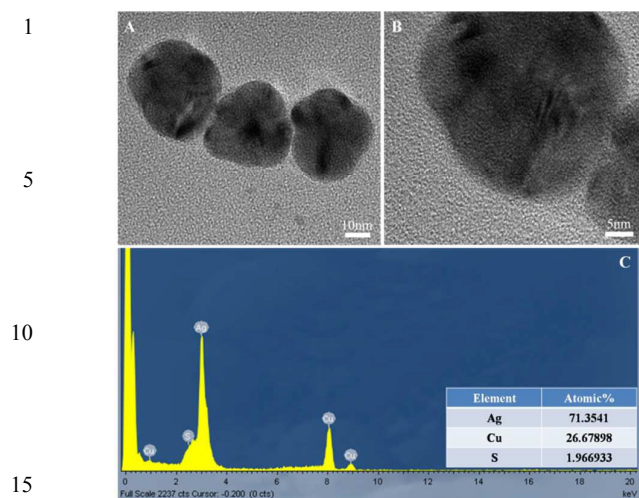


**Fig. 3** The characterizations of AgNPs after exposure to NaDDC aqueous solution for 10 min: (A) HRTEM image of AgNPs, (B) further magnified HRTEM image and (C) EDS spectrum of AgNPs after the completion with NaDDC.

of NaDDC, and makes chemical equilibrium shift to the right continuously.

#### Concentration-dependent degradation of NaDDC in both neutral and alkaline conditions

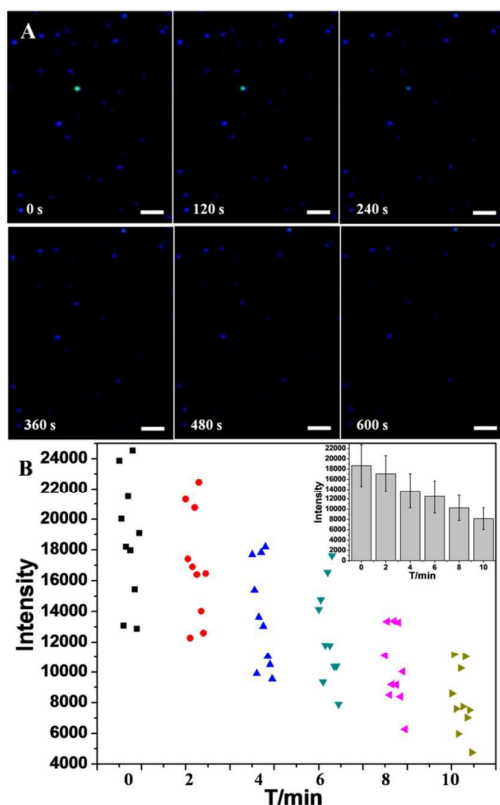


**Fig. 4** Scattered light iDFM of AgNPs after the 0.5 mM NaDDC aqueous solution added into the cell (A) and the scattering intensity statistics of the chosen 10 AgNPs over time (B). The insert showed the changes in the total intensity of AgNPs. The scale bar corresponds to 2  $\mu$ m for all images.

In order to identify that the release of  $S^{2-}$  resulted from the reaction in neutral and alkaline conditions, both 0.5 mM and 1.0 mM of NaDDC were tested. This reaction was NaDDC-concentration dependent. Compared with 1 mM NaDDC solution (Fig. 2), with the addition of 0.5 mM NaDDC aqueous solution, the reaction progress proceeded much milder, and no color change, but the scattering intensity of AgNPs declined over time (Fig. 4A). Fig. 4B showed the scattering intensity statistics of the chosen 10 AgNPs in 0, 2, 4, 6, 8, 10 time point, which intuitively indicated the change trends of scattering intensity. The whole degradation process became longer as well in this concentration, and it ended after about 20 minutes. The scattering light intensity of AgNPs in Fig. 5D did not change any more, showing the termination of reaction.

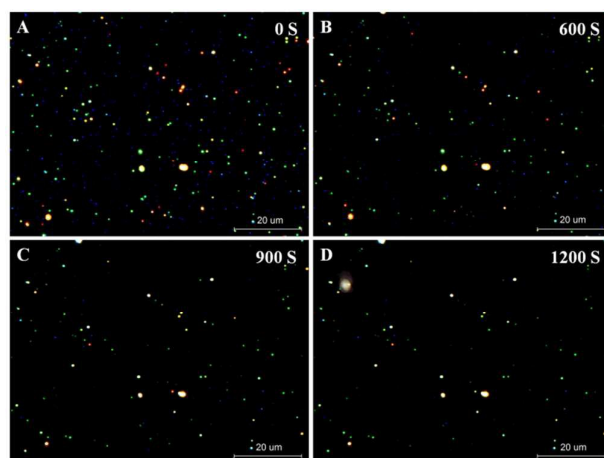


**Fig. 5** Light scattering iDFMs of AgNPs of the same area after the addition of 0.5 mM NaDDC aqueous solution at 0 s, 600 s, 900 s and 1200 s.

0.5 mM NaDDC alkaline solution was applied to show the differences compared to neutral condition (Fig. 6). The reaction was more intense and unlike the neutral solution, 0.5 mM NaDDC alkaline solution could make the scattering light color of some AgNPs gradually change from blue to green, with a more obvious decline in light intensity.

If increasing the concentration of NaDDC alkaline solution to 1 mM, its reaction with AgNPs was too intense that the overall

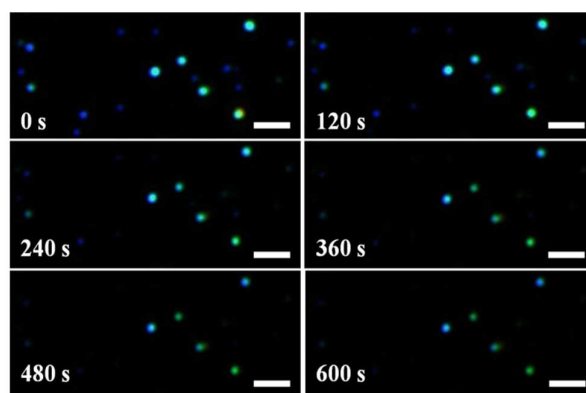


**Fig. 6** Light scattering iDFMs of AgNPs after the 0.5 mM NaDDC alkaline solution (pH, 9) added into the cell. The scale bar is 2  $\mu$ m for all images.

1 morphology of AgNPs in the bottom changed a lot (Fig. S2†), and most of them disappeared after reaction. That is to say, NaDDC could produce more S<sup>2-</sup> after degradation in alkaline condition and when the concentration of NaDDC reached a certain value, it could change the scattering light color of AgNPs. DFM images before and after reaction at pH 7 and 9 were captured to show the difference in neutral and alkaline conditions (Fig. S3†).

5 The scattering light color change of the AgNPs should be ascribed to the wavelength shifts with the reaction process (Fig. 7). The scattering spectrum of the same AgNP before and after reaction with 1 mM NaDDC was also measured and it underwent a redshift from 471 nm to 526 nm (Fig. 7A). When 0.5mM NaDDC aqueous solution was employed, the reaction became milder and the scattering light had little color change, with a spectral redshift about 27.5 nm (Fig. 7B). When 0.5mM NaDDC alkaline solution was employed, the scattering light color of AgNPs underwent a color change, and the spectrum shifted from 447 nm to 497.5 nm (Fig. 7C). The more redshift of the scattering light of AgNPs in alkaline condition indicated that there were more Ag<sub>2</sub>S generated on the surface of AgNP compared to neutral condition. Namely, NaDDC could decompose more intensively and produce more S<sup>2-</sup> in alkaline condition, which supported our deduction considering that OH<sup>-</sup> was the major reactant in the decomposition reaction of NaDDC.

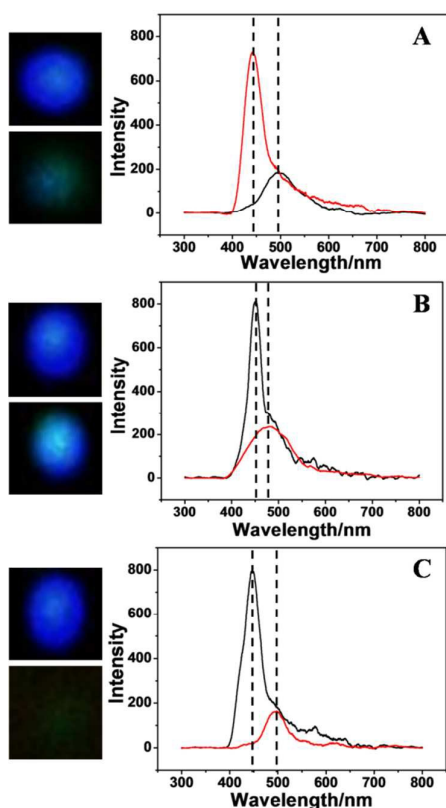
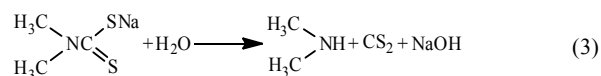


Fig. 7 The scattering spectral changes of AgNPs before and after the 1 mM aqueous (A), 0.5 mM aqueous (B) and 0.5 mM alkaline (C) NaDDC solution added into the cell, respectively. The dark field microscopic images and corresponding resonant scattering spectra of the chosen Ag nanoparticles before (black curves) and after (red curves) their exposure to NaDDC solution for 10 min.

### Real-time monitoring of the degradation of NaDDC

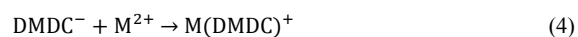
Then the *in situ* degradation of NaDDC was real-time monitored. Its degradation in acid condition has been researched, and the mechanisms of decomposition can be described as equation 3:<sup>24</sup>



Thus the acid decomposition was not involved. Here we considered reactions at pH 7 and pH 9. With the addition of 1 mM NaDDC aqueous solution at pH 7, the scattering light color of AgNPs gradually changed from blue to green, with an obvious decline in light intensity, even if the scattering light of some AgNPs disappeared (Movie. 1†). In contrast, with the addition of 1 mM NaDDC PB solution at pH 9, the reaction became more intense and the scattering light color of AgNPs changed from blue to green more quickly, most of them disappeared after the reaction (Movie. 2†). Other concentrations were used to try and the 10 μM NaDDC aqueous solution was the lowest concentration which could cause the scattering light intensity change of AgNPs (Fig. S4†).

### The complexation between NaDDC and metal ions

Metal ions, for example the copper (II) ions, could generate a 2:1 complex with NaDDC, thus inhibiting its degradation. The resulting complex was very stable and would not produce any toxic substances. NaDDC had also been commercially used as metal-chelator for this reason. The following reactions between metals and dimethyldithiocarbamate (DMDC) occur in equation 4 and 5 as:<sup>49</sup>



However, the dosage of NaDDC was difficult to control in the chelation. The application of DFM could resolve this problem. If NaDDC was overfeeding, the remaining NaDDC in solution could continue to change the scattering light of AgNPs after chelation, which could be intuitively observed by DFM.

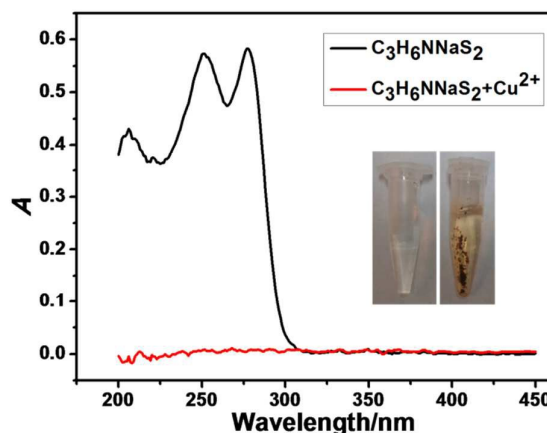


Fig. 8 The UV absorption spectrum of NaDDC solution before and after the addition of CuSO<sub>4</sub>. The insert showed the photographs of NaDDC solution with (right) or without (left) the addition of half the amount of CuSO<sub>4</sub>.

1 Considering that the complex of  $\text{Cu}^{2+}$  and NaDDC was the most stable,<sup>50</sup> copper (II) ions were selected for experiment. When 0.5 mM  $\text{CuSO}_4$  solution was added to the 1 mM NaDDC solution, there were many brown precipitates produced (Fig. S5†). After centrifugation, the supernatant was taken for UV absorption measurement (Fig. 8). The absorption peaks at 251 nm and 277 nm disappeared, indicating the NaDDC in solution was removed. The UV absorption spectrums before and after complexation in neutral, acid and alkaline conditions were presented in Fig. S6† respectively, and the results showed the complexation between  $\text{Cu}^{2+}$  and NaDDC could happen irrespective of pH.

Then we added the supernatant into the simulated flow cell for dark-field imaging, to see if it could make changes on the scattering of AgNPs. As shown in the DFM images in Fig. 9A, the scattering light of AgNPs did not change. The intensity statistics by IPP (Fig. 9B) also supported this consequence. The complexation of  $\text{Zn}^{2+}$  and NaDDC was also investigated (Fig. S7†), and the results showed  $\text{Zn}^{2+}$  could inhibit the decomposition of NaDDC.

To investigate the stoichiometric ratio between NaDDC and  $\text{Cu}^{2+}$ , three sets of solution (The ratio of the amount of NaDDC and  $\text{Cu}^{2+}$

was 4:1, 2:1 and 1:1 respectively) were prepared, in which 1 mM NaDDC aqueous solution and 0.25 mM, 0.5 mM, 1 mM  $\text{CuSO}_4$  aqueous solution were employed correspondingly. Upon mixed, they reacted and produced many brown precipitates. Removing the precipitates by centrifugation and drawing the supernatant into the flow cell, the dynamic images of the reaction were taken by DFM. The supernatant of the first group (NaDDC: $\text{Cu}^{2+}$  = 4:1) could still change the scattering light intensity of AgNPs, showing  $\text{Cu}^{2+}$  could not inhibit the hydrolysis of NaDDC thoroughly in this ratio (Fig. S8†), and thus proving the feasibility of applying DFM to estimate whether NaDDC was excessive when used in metal removal.

The supernatant of the second group could not change the scattering light of AgNPs, showing in this ratio  $\text{Cu}^{2+}$  and NaDDC completely complexed (Fig. 9). The result was the same with former when excess  $\text{Cu}^{2+}$  ions (the third group) were employed to inhibit the hydrolysis of NaDDC (Fig. S9†). The stoichiometric ratio between NaDDC and  $\text{Cu}^{2+}$  was 2:1. The inhibition of  $\text{Cu}^{2+}$  in alkaline condition was also investigated (Fig. S10†), and the result showed  $\text{Cu}^{2+}$  could inhibit the hydrolysis of NaDDC in this condition. The stability of the complex of  $\text{Cu}^{2+}$  and NaDDC was also investigated by adding the reaction solution into the flow cell without centrifugation, and the results showed that the complex was stable and could not induce the change of the scattering light of AgNPs (Fig. S11†).

## Conclusions

In summary, we achieved a real-time monitoring of the dynamic degradation process of NaDDC by DFM and deduced the chemical formulas of the degradation, expanding SNA technique to a new field. As far as we know, it is also for the first time to research the degradation dynamics of NaDDC in neutral and alkaline conditions. The reaction between NaDDC and AgNPs didn't have specific regulation, but through RGB analysis and scanning spectrum before and after reaction we developed a semi-quantitative detection method of NaDDC. The minimum response concentration was 10  $\mu\text{M}$ , lower than the conventional methods. The pesticide could change the intensity as well as the color of AgNPs, making the process of degradation visual and easy to analyze. Besides NaDDC, our method could also be utilized to monitor the decomposition reactions of other pesticides. The HRTEM images were taken to prove the formation of  $\text{Ag}_2\text{S}$  on the surface of the AgNPs. The whole decomposition process of NaDDC was monitored in nanoscale.

The other work was to study whether the metal ions could inhibit the neutral- and alkaline-hydrolysis of NaDDC. The result showed they could and the ratio of NaDDC and  $\text{Cu}^{2+}$  ions was 2:1, so we could declare that the inhibition of metal ions on the degradation of NaDDC was irrespective of pH. Our strategy visualized the NaDDC present in solution and added benefits to resolving the problem of overfeeding in NaDDC use. These conclusions could help understanding and defining this kind of degradation mechanisms and contribute to reducing or eliminating the hazards of NaDDC.

## Acknowledgements

This work was financially supported by the National Natural Science Foundation of China (NSFC, No. 21535006).

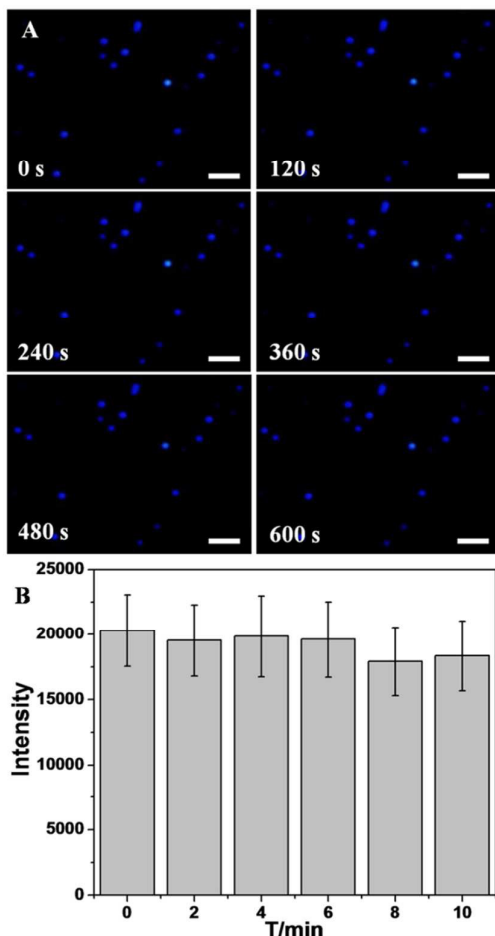


Fig. 9 Scattered light iDFM of AgNPs after the supernatant (NaDDC: $\text{Cu}^{2+}$  = 2:1) added into the cell (A). The scattering intensity of the chosen AgNPs remained the same before and after the reaction, accompanied with a small mechanical error (B). The scale bar corresponds to 2  $\mu\text{m}$  for all images.

1 **Notes and references**

<sup>a</sup> Key Laboratory of Luminescent and Real-Time Analytical Chemistry (Southwest University), Ministry of Education, College of Pharmaceutical Sciences, Southwest University, Chongqing 400716, P. R. China.

<sup>b</sup>Chongqing Key Laboratory of Biomedical Analysis (Southwest University), Chongqing Science & Technology Commission, College of Chemistry and Chemical Engineering, Southwest University, Chongqing 400715, China

† Electronic Supplementary Information (ESI) available: [additional DFM images (Fig.S1-S9) and the typical dynamic iDFM of monitoring (Movie S1-S2)]. See DOI: 10.1039/b000000x/

- 10 1. A. J. Haes, L. Chang, W. L. Klein and R. P. Van Duyne, *J. Am. Chem. Soc.*, 2005, **127**, 2264-2271.
2. Y. Choi, Y. Park, T. Kang and L. P. Lee, *Nat. Nanotechnol.*, 2009, **4**, 742-746.
- 15 3. X.-L. Hu, H.-Y. Jin, X.-P. He, T. D. James, G.-R. Chen and Y.-T. Long, *ACS Appl. Mater. Interfaces*, 2015, **7**, 1874-1878.
4. Z. Chen, J. Li, X. Chen, J. Cao, J. Zhang, Q. Min and J.-J. Zhu, *J. Am. Chem. Soc.*, 2015, **137**, 1903-1908.
- 20 5. L. Zhang, Y. Li, D.-W. Li, C. Jing, X. Chen, M. Lv, Q. Huang, Y.-T. Long and I. Willner, *Angew. Chem. Int. Edit.*, 2011, **50**, 6789-6792.
- 25 6. L. P. Wu, Y. F. Li, C. Z. Huang, Q. Zhang, *Anal. Chem.*, 2006, **78**, 5570-5577.
7. C. Z. Huang, K. A. Li, S. Y. Tong, *Anal. Chem.*, 1996, **68**, 2259-2263.
8. Y. Liu and C. Z. Huang, *ACS Nano*, 2013, **7**, 11026-11034.
- 30 9. L. Shi, C. Jing, W. Ma, D.-W. Li, J. E. Halls, F. Marken and Y.-T. Long, *Angew. Chem. Int. Edit.*, 2013, **52**, 6011-6014.
10. H. Yang, Y. Liu, P. F. Gao, J. Wang and C. Z. Huang, *Analyst*, 2014, **139**, 2783-2787.
- 35 11. T. Xie, C. Jing, W. Ma, Z. Ding, A. J. Gross and Y.-T. Long, *Nanoscale*, 2015, **7**, 511-517.
- 40 12. S. Singh, R. Gupta and S. Sharma, *J. Hazard. Mater.*, 2015, **291**, 102-110.
13. D. Pimentel and M. Burgess, *Environ. Dev. Sustainabil.*, 2012, **14**, 1-2.
- 45 14. S. B. Emery, A. Hart, C. Butler-Ellis, M. G. Gerritsen-Ebben, K. Machera, P. Spanoghe and L. J. Frewer, *Hum. Ecol. Risk Assess.*, 2014, **21**, 1062-1080.
15. Y. Zhan and M. H. Zhang, *Sci. Total Environ.*, 2014, **472**, 517-529.
- 50 16. Y. Liu and C. Z. Huang, *Chem. commun.*, 2013, **49**, 8262-8264.

17. W.-G. Qu, B. Deng, S.-L. Zhong, H.-Y. Shi, S.-S. Wang and A.-W. Xu, *Chem. commun.*, 2011, **47**, 1237-1239.
18. S. Berciaud, L. Cognet, P. Tamarat and B. Lounis, *Nano letters*, 2005, **5**, 515-518.
19. A. D. McFarland and R. P. Van Duyne, *Nano letters*, 2003, **3**, 1057-1062.
20. Y. Luo, S. Shen, J. Luo, X. Wang and R. Sun, *Nanoscale*, 2015, **7**, 690-700.
21. V. Tharmaraj and J. Yang, *Analyst*, 2014, **139**, 6304-6309.
22. J. M. Goldman, A. S. Murr, A. R. Buckalew and R. L. Cooper, *Toxicol. Sci.*, 2008, **104**, 107-112.
23. K. I. Aspila, V. S. Sastri and C. L. Chakrabarti, *Talanta*, 1969, **16**, 1099-1102.
24. L. E. Lopatecki and W. Newton, *Can. J. Bot.*, 1952, **30**, 131-138.
25. E. Humeres, N. A. Debacher, M. M. d. S. Sierra, J. D. Franco and A. Schutz, *J. Org. Chem.*, 1998, **63**, 1598-1603.
26. S. J. Joris, K. I. Aspila and C. L. Chakrabarti, *Anal. Chem.*, 1970, **42**, 647-651.
27. M. Kulka, *Can. J. Chem.*, 1956, **34**, 1093-1100.
28. H. M. Dekhuijzen, *Nature*, 1961, **191**, 198-199.
29. M. M. Matlock, K. R. Henke and D. A. Atwood, *J. Hazard. Mater.*, 2002, **92**, 129-142.
30. M. J. McFarland, C. Glarborg and M. A. Ross, *Water. Environ. Res.*, 2012, **84**, 2086-2089.
31. C. A. Erven, *Met. Finish.*, 2001, **99**, 8-19.
32. W. A. Mitch and D. L. Sedlak, *Environ. Sci. Technol.*, 2004, **38**, 1445-1454.
33. C. Lee, W. Choi, Y. G. Kim and J. Yoon, *Environ. Sci. Technol.*, 2005, **39**, 2101-2106.
34. T. Yamase, H. Kokado and E. Inoue, *B. Chem. Soc. Jpn.*, 1970, **43**, 934-935.
35. X. Z. Cao and Y. M. Li, *Anal. Methods*, 2012, **4**, 2996-3001.
36. A. J. Nitowski, A. A. Nitowski, J. A. Lent, D. W. Bairley and D. Van Valkenburg, *J. Chromatogr. A*, 1997, **781**, 541-545.
37. J. G. Smith, Q. Yang and P. K. Jain, *Angew. Chem. Int. Edit.*, 2014, **53**, 2867-2872.
38. D. Steinigeweg and S. Schlucker, *Chem. commun.*, 2012, **48**, 8682-8684.
39. S. Lilienfeld and C. E. White, *J. Am. Chem. Soc.*, 1930, **52**, 885-892.

Journal Name	ARTICLE
40. J. Zeng, J. Tao, D. Su, Y. Zhu, D. Qin and Y. N. Xia, <i>Nano letters</i> , 2011, 11, 3010-3015.	1
1 41. C. H. Fang, Y. H. Lee, L. Shao, R. B. Jiang, J. F. Wang and Q.-H. Xu, <i>ACS Nano</i> , 2013, 7, 9354-9365.	1 5
42. Y. Liu and C. Z. Huang, <i>Nanoscale</i> , 2013, 5, 7458-7466.	5
5 43. P. K. Jain, X. Huang, I. H. El-Sayed and M. A. El-Sayed, <i>Accounts Chem. Res.</i> , 2008, 41, 1578-1586.	5
44. J. Hao, B. Xiong, X. Cheng, Y. He and E. S. Yeung, <i>Anal. Chem.</i> , 2014, 10 86, 4663-4667.	10 10
45. B. Xiong, R. Zhou, J. Hao, Y. Jia, Y. He and E. S. Yeung, <i>Nat. Commun.</i> , 15 2013, 4, 1708.	15
15 46. P. D. Nallathamby, T. Huang and X.-H. N. Xu, <i>Nanoscale</i> , 2010, 2, 1715-1722.	15
47. C. Burda, X. Chen, R. Narayanan and M. A. El-Sayed, <i>Chem. Rev.</i> , 2005, 20 105, 1025-1102.	20 20
48. I. Choi, H. D. Song, S. Lee, Y. I. Yang, T. Kang and J. Yi, <i>J. Am. Chem. Soc.</i> , 2012, 134, 12083-12090.	25
25 49. K. W. Weissmahr and D. L. Sedlak, <i>Environ. Toxicol. Chem.</i> , 2000, 19, 25 820-826.	25 25
50. M. Hallaway, <i>Biochim. Biophys. Acta</i> , 1959, 36, 3.	30
30 30	30 30
35 35	35 35
40 40	40 40
45 45	45 45
50 50	50 50
50 50	50 50
55 55	55 55
55 55	55 55

## Graphic abstract

for

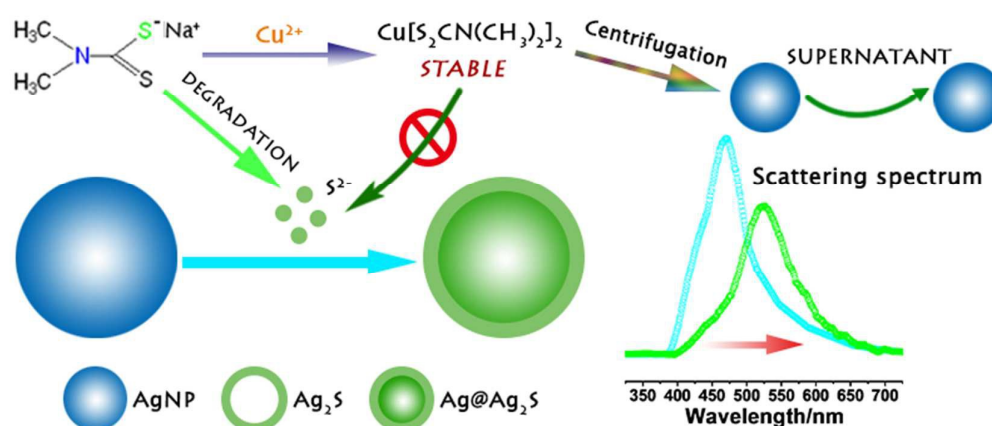
# Real-time scattered light dark-field microscopic imaging of the dynamic degradation process of sodium dimethyldithiocarbamate

Gang Lei,<sup>a</sup> Peng Fei Gao,<sup>a</sup> Hui Liu,\*<sup>a</sup> and Cheng Zhi Huang \*<sup>a b</sup>

<sup>a</sup> Key Laboratory of Luminescent and Real-Time Analytical Chemistry (Southwest University), Ministry of Education, College of Pharmaceutical Sciences, Southwest University, Chongqing 400716, P. R. China.

<sup>b</sup> School of Chemistry and Chemical Engineering, Southwest University, Chongqing 400715, P. R. China.

\* Corresponding Author. E-mail: [chengzhi@swu.edu.cn](mailto:chengzhi@swu.edu.cn)



Quantitatively real-time monitoring of the dynamic degradation process of NaDDC in neutral and alkaline conditions and the inhibition effects of metal ions were made by using single nanoparticle analysis technique with the aid of dark field microscopic imaging (iDFM), and a chemical mechanism of the degradation of NaDDC in neutral and alkaline conditions was proposed, and the inhibit effects of metal ions including Zn (II) and Cu (II) were investigated in order to understand the decomposition process in environments.

**Electronic Supplementary Information (ESI)***for***Real-time scattered light dark-field microscopic imaging of the dynamic degradation process of sodium dimethyldithiocarbamate**Gang Lei,<sup>a</sup> Peng Fei Gao,<sup>a</sup> Hui Liu, \*<sup>a</sup> and Cheng Zhi Huang \*<sup>a b</sup><sup>a</sup> Key Laboratory of Luminescent and Real-Time Analytical Chemistry (Southwest University), Ministry of Education, College of Pharmaceutical Sciences, Southwest University, Chongqing 400716, P. R. China.<sup>b</sup> Chongqing Key Laboratory of Biomedical Analysis (Southwest University), Chongqing Science & Technology Commission, College of Chemistry and Chemical Engineering, Southwest University, Chongqing 400715, China

\* Corresponding Author. E-mail: chengzhi@swu.edu.cn

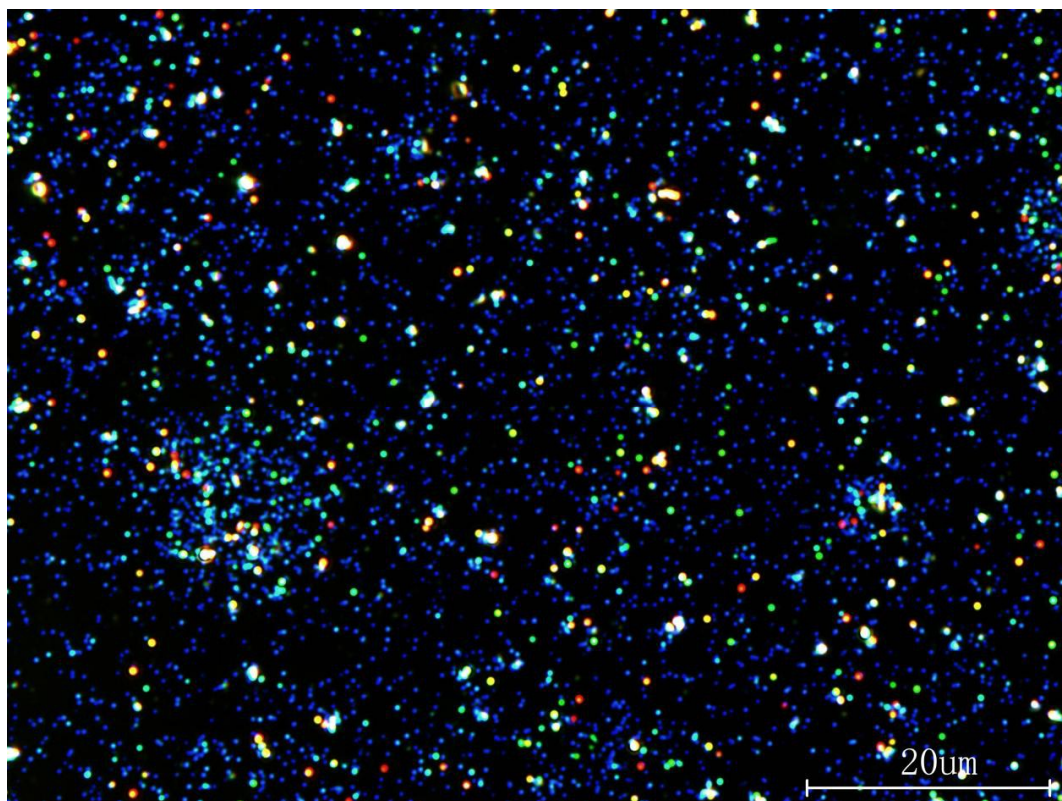


**Fig. S1** Scattered light iDFMs of AgNPs synthesized with a 100-time dilution. The image scale bar corresponds to 20  $\mu\text{m}$ .

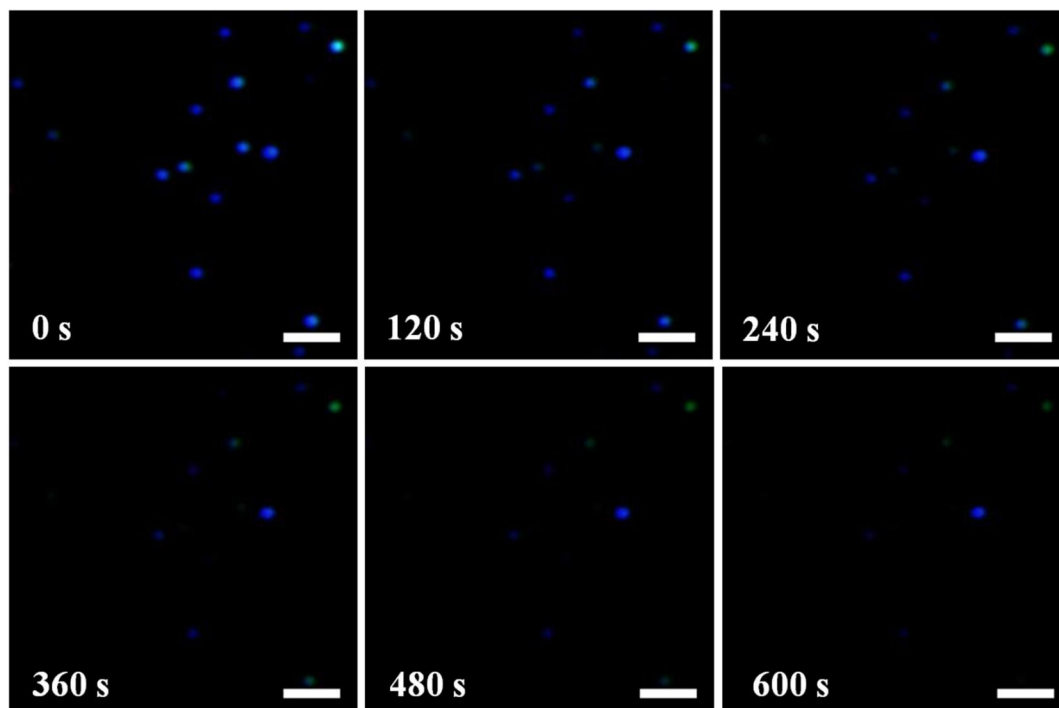


**Fig. S2** Scattered light iDFMs of AgNPs after the 1 mM NaDDC alkaline solution (pH, 9) added into the cell. The scale bar is 2  $\mu\text{m}$  for all images.

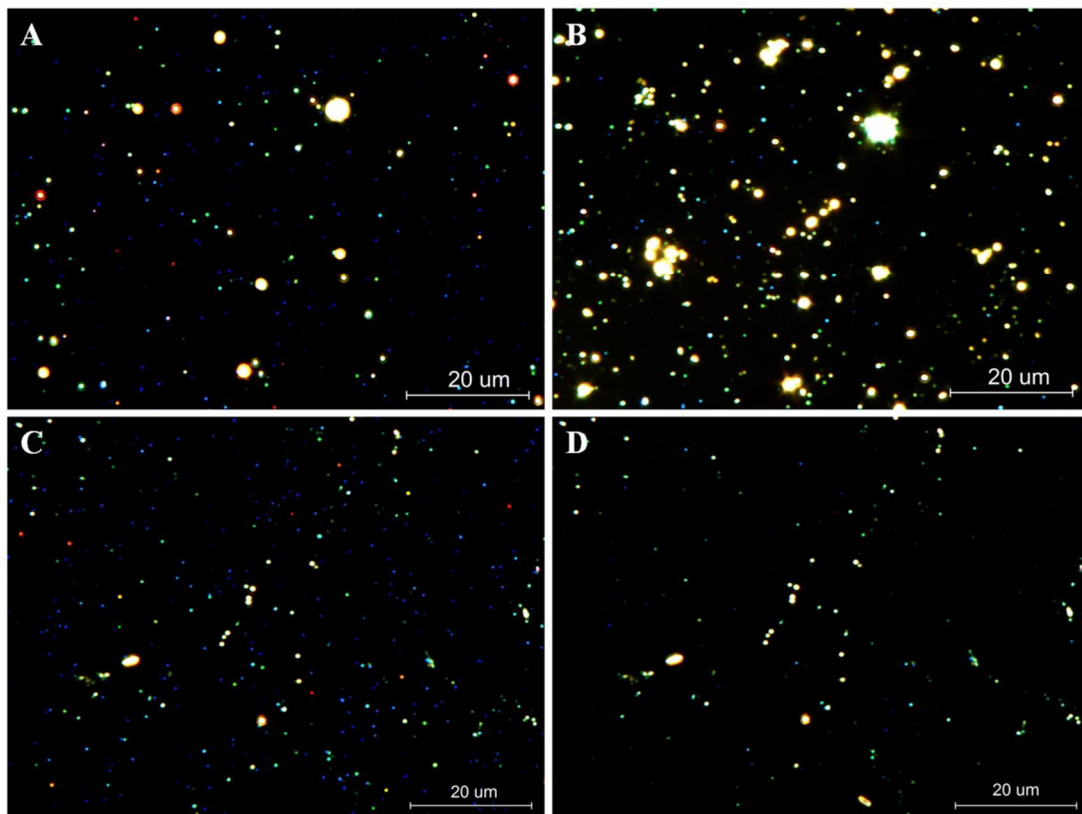


**Fig. S3** Scattered light iDFMs of AgNPs of the same area before (A, C) and after (B, D) the reaction with 1 mM NaDDC in neutral (A, B) and alkaline (C, D) conditions.

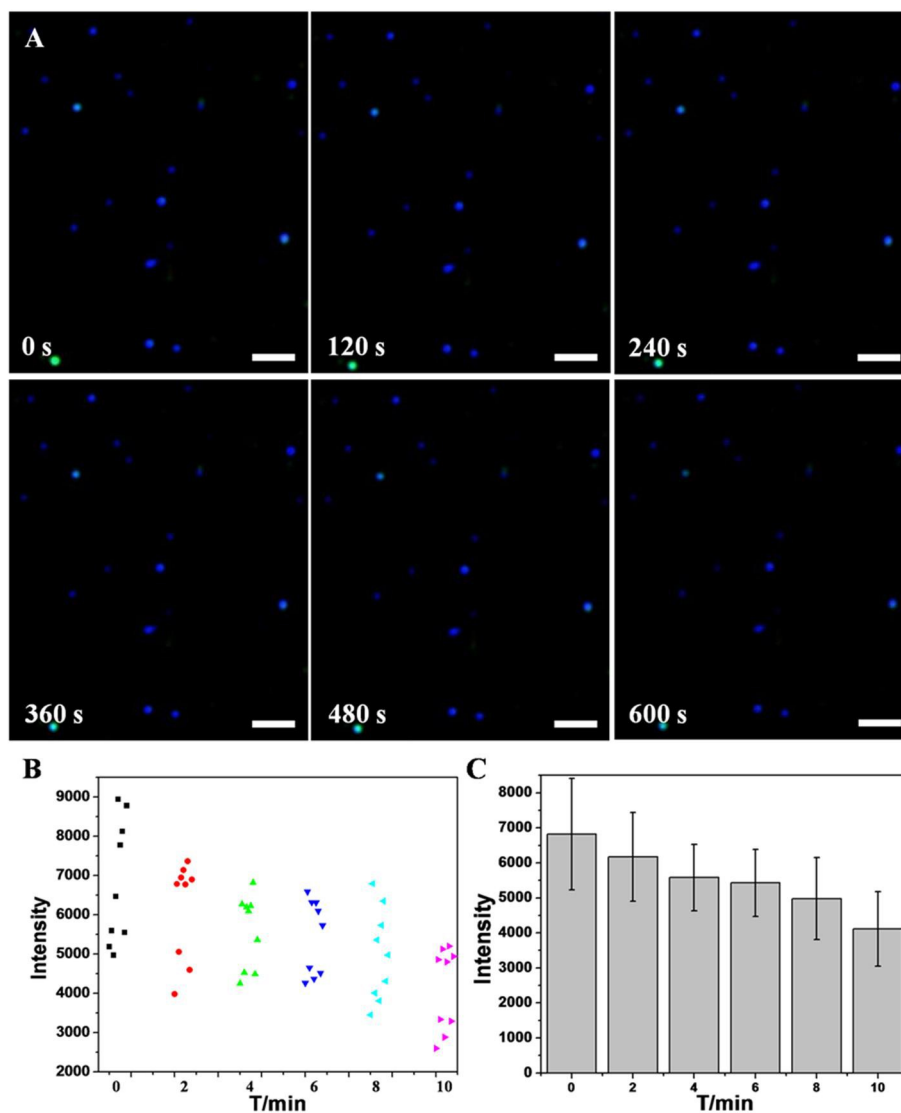


**Fig. S4** Scattered light iDFMs of AgNPs after the 10  $\mu\text{M}$  NaDDC aqueous solution added into the cell (A), the scattering light intensity statics of the chosen AgNPs (B) and the average intensity with error bar (C). The scale bar is 2  $\mu\text{m}$  for all images.

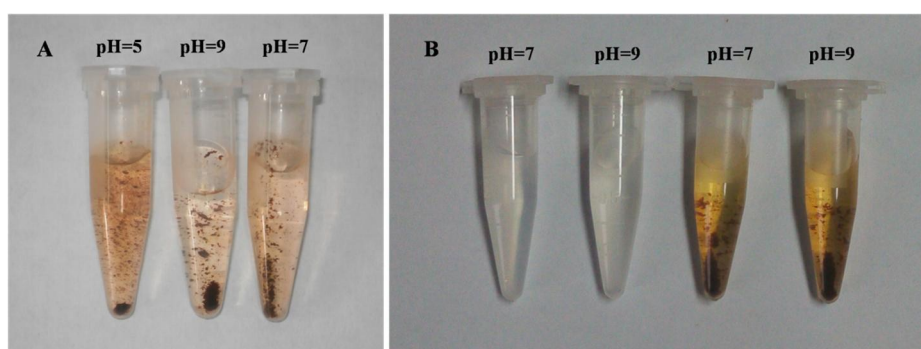


**Fig. S5** Photographs of complex formed by  $\text{Cu}^{2+}$  and NaDDC at different pH (A) and photographs of complex formed by  $\text{Zn}^{2+}$  and NaDDC (left, white precipitate),  $\text{Cu}^{2+}$  and NaDDC (right, brown precipitate) at different pH (B). The ratio of metal ions and NaDDC is 1:2.  $\text{C}_3\text{H}_6\text{NNaS}_2$ ,  $1 \times 10^{-3} \text{ mol L}^{-1}$ .

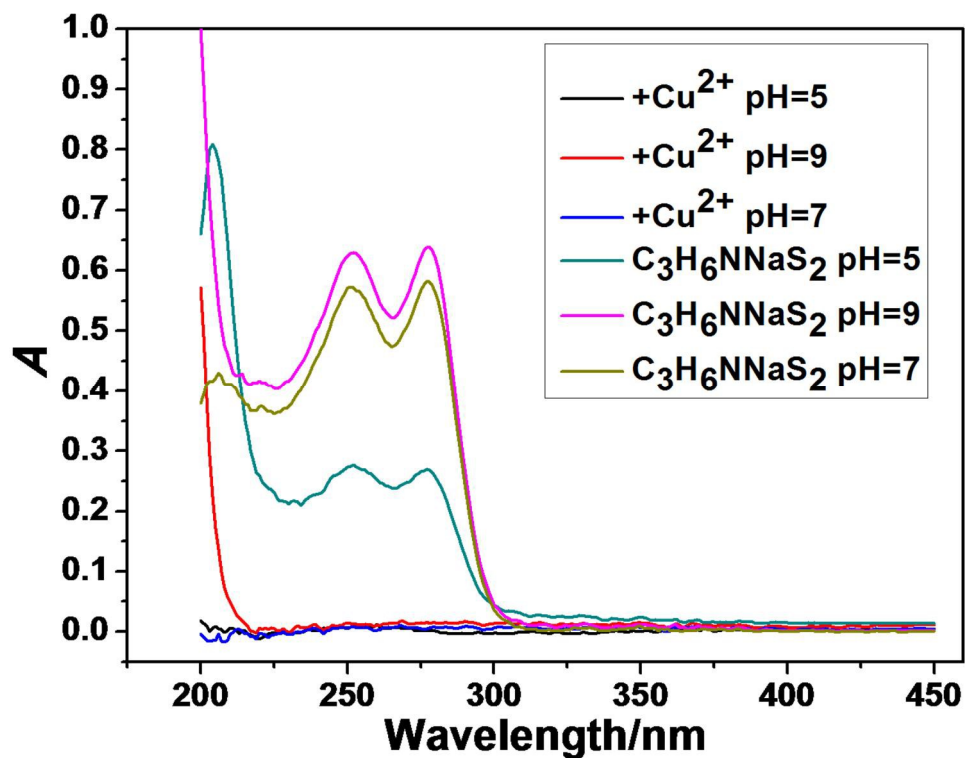


**Fig. S6** The UV absorption spectrums of NaDDC before and after complexation in neutral, acid and alkaline condition respectively.

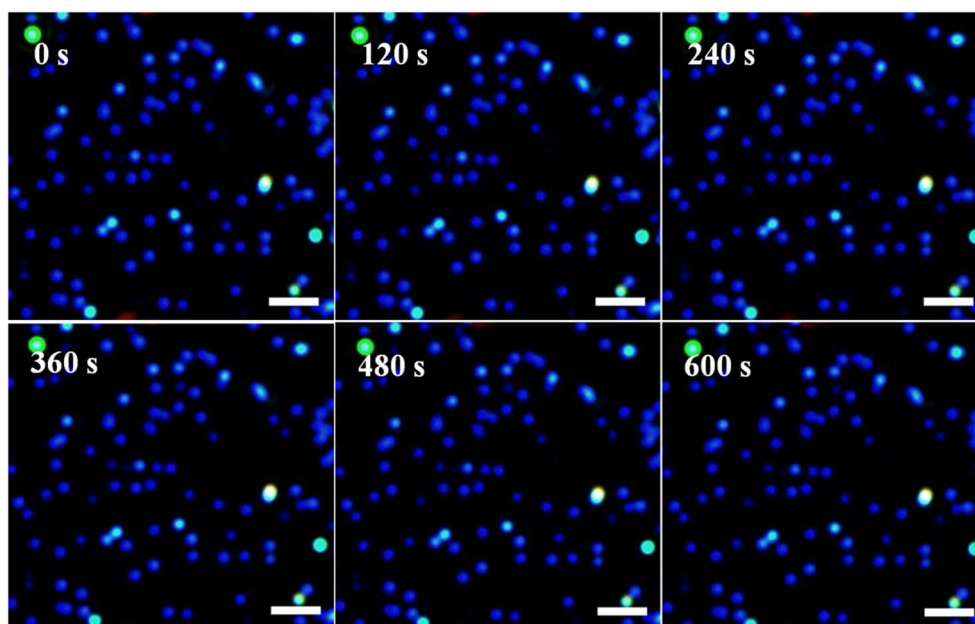


**Fig. S7** The influence on the scattered light of AgNPs by the supernatant of mixed solution of Zn<sup>2+</sup> and NaDDC. The result showed that it could not change the scattering light of AgNPs. The ratio of Zn<sup>2+</sup> and NaDDC is 1:2, and the scale bar is 2  $\mu$ m for all images.

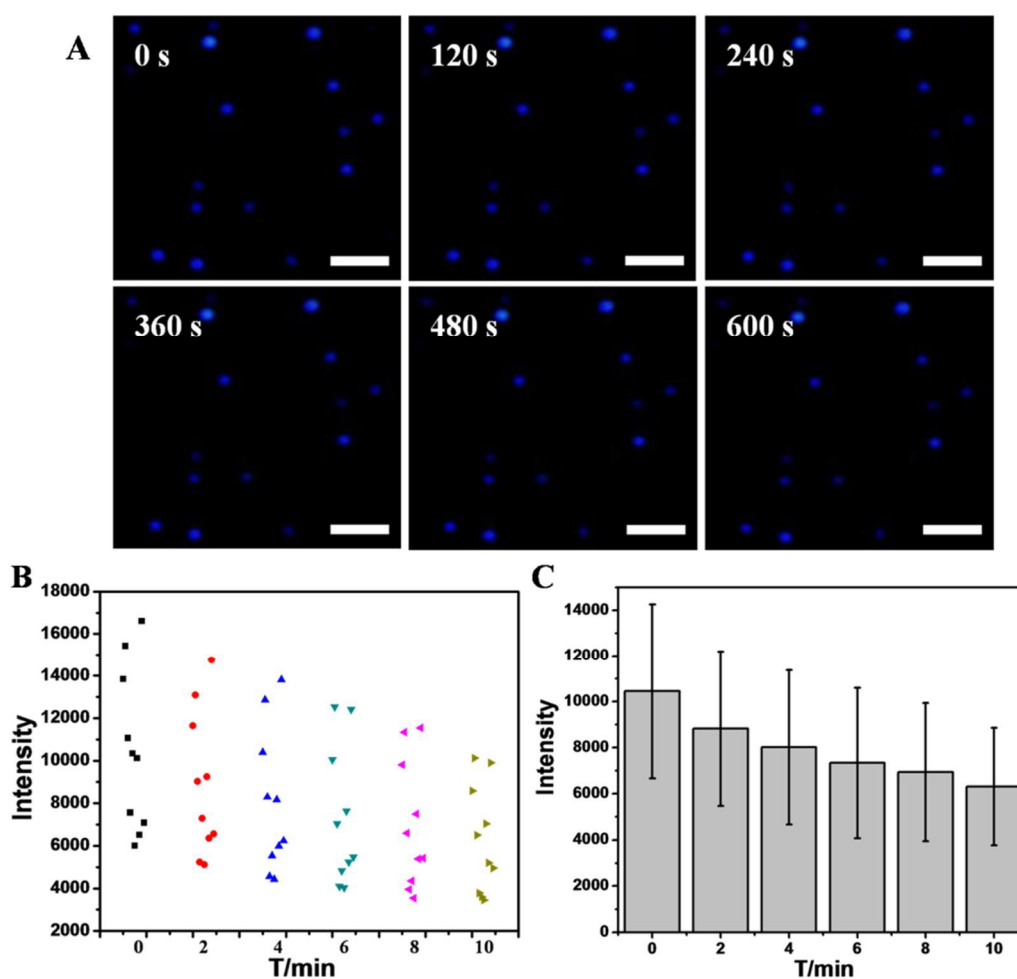


**Fig. S8** Scattered light iDFMs of AgNPs after the supernatant (NaDDC:Cu<sup>2+</sup> = 4:1) added into the cell (A), the scattering light intensity statics of the chosen AgNPs (B) and the average intensity with error bar (C). The scale bar is 2  $\mu$ m for all images.

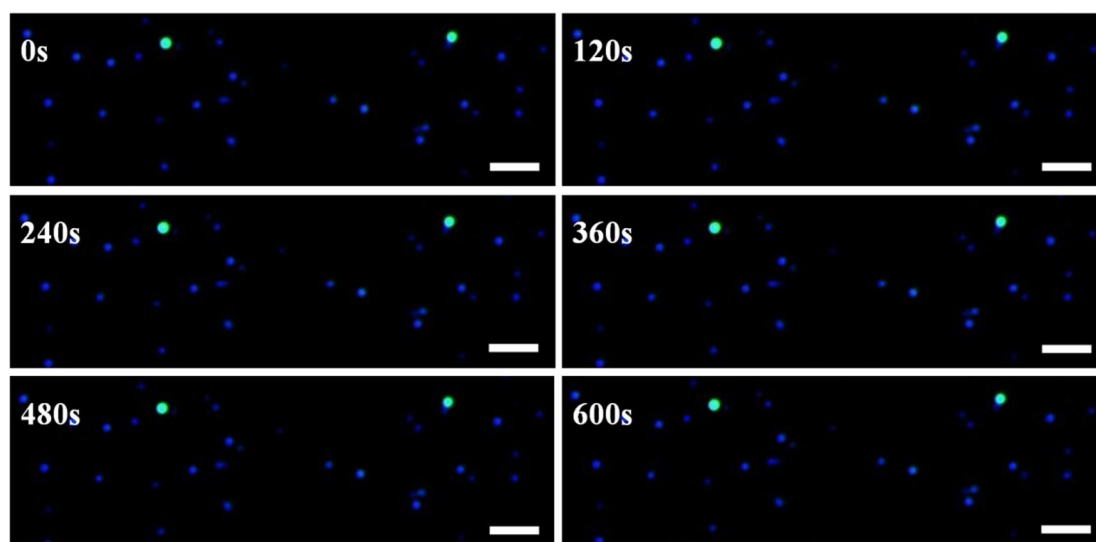


**Fig. S9** The influence on the scattered light of AgNPs by the supernatant of mixed solution of Cu<sup>2+</sup> ions and NaDDC. The ratio of Cu<sup>2+</sup> ions and NaDDC is 1:1, and the scale bar is 2  $\mu$ m for all images.

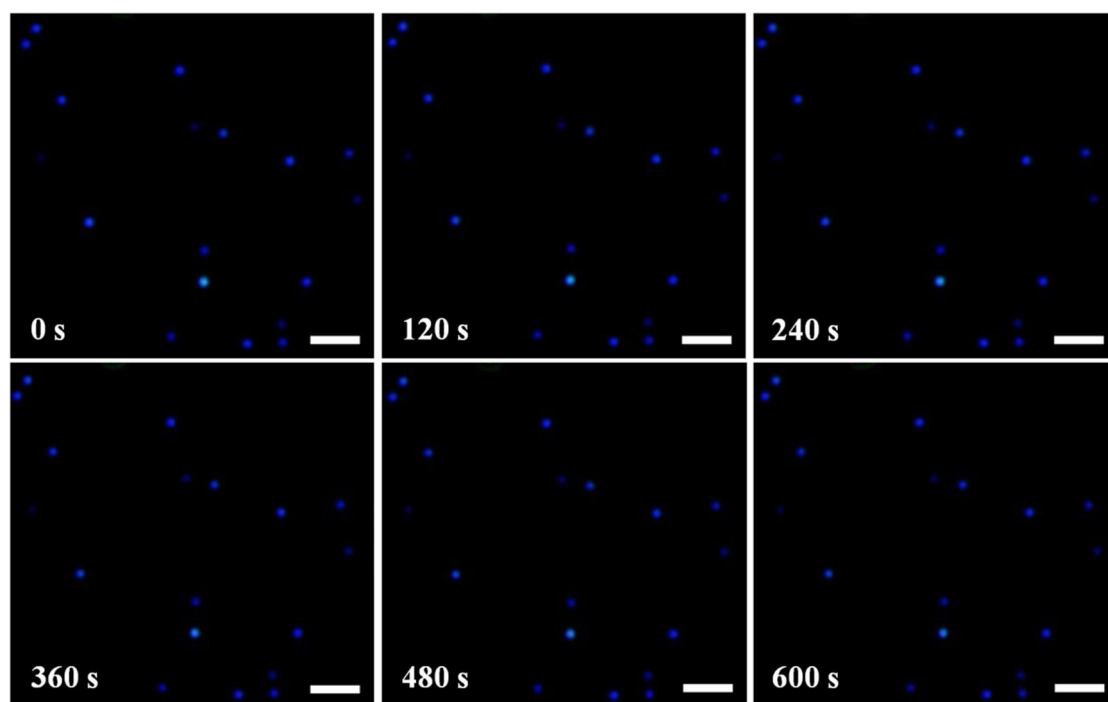


**Fig. S10** The influence on the scattered light of AgNPs by the supernatant of mixed solution of  $\text{Cu}^{2+}$  and NaDDC in alkaline condition. The ratio of  $\text{Cu}^{2+}$  and NaDDC is 1:2, and the scale bar is 2  $\mu\text{m}$  for all images.

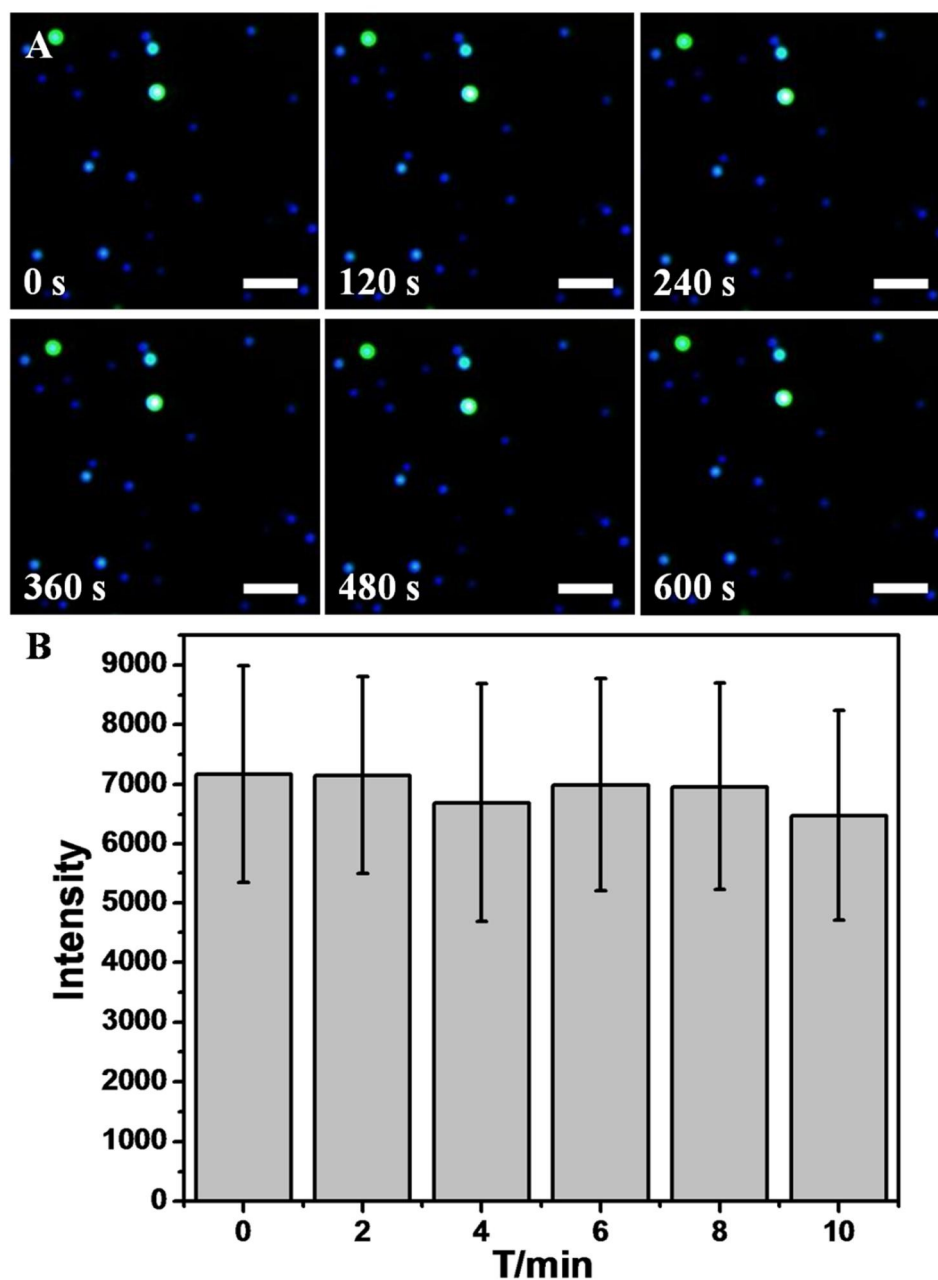


**Fig. S11** Scattered light iDFMs of AgNPs after the complex of NaDDC and  $\text{Cu}^{2+}$  added into the cell (A). The scattering intensity of the chosen AgNPs remained the same before and after the reaction, accompanied with a small mechanical error (B). The scale bar corresponds to  $2 \mu\text{m}$  for all images.



Journal Name

ARTICLE

# Real-time scattered light dark-field microscopic imaging of the dynamic degradation process of sodium dimethyldithiocarbamate

Gang Lei,<sup>a</sup> Peng Fei Gao,<sup>a</sup> Hui Liu\*<sup>a</sup>, and Cheng Zhi Huang\*<sup>a,b</sup>

Received 00th January 20xx,  
Accepted 00th January 20xx

DOI: 10.1039/x0xx00000x

www.rsc.org/

Single nanoparticle analysis (SNA) technique has caused wide attention with the aid of dark-field microscopic imaging (iDFM) technique owing to its high sensitivity. Considering that the degradation of pesticides can bring about serious problems in food and environment and real-time monitoring the dynamic degradation process of pesticides can help understanding and defining their degradation mechanisms, herein we made real-time monitoring of the decomposition dynamics of sodium dimethyldithiocarbamate (NaDDC) in neutral and alkaline conditions by imaging single silver nanoparticles (AgNPs) under a dark-field microscope (DFM) by taking this pesticide as an example, in which the localized surface plasmon resonance (LSPR) scattering signals were measured at single nanoparticle level. As a result, the chemical mechanism of the degradation of NaDDC in neutral and alkaline conditions was proposed, and the inhibit effects of metal ions including Zn (II) and Cu (II) were investigated in order to understand the decomposition process in environments. It was found that Cu (II) can form a most stable complex with NaDDC with a stoichiometric ratio of 2:1, greatly reduces the toxicity.

## Introduction

Single nanoparticle analysis (SNA) technique, developed by using the localized surface plasmon resonance (LSPR) scattering signals of single noble metal nanoparticles by dark-field microscopic imaging (iDFM), has attracted much attention and has been widely employed in biosensing, chemical detection and cellular imaging in recent years.<sup>1-4</sup> SNA technique is more accurate than conventional analytical methods because every single nanoparticle can serve as an independent sensor in iDFM.<sup>5</sup> For example, resonance light scattering technique in solution has been widely applied for analytical purposes, wherein the signals measured for analysis were obtained from an ensemble of nanoparticles or aggregates.<sup>6,7</sup> We noticed that one of the important research fields of SNA technique is to be applied for the real-time monitoring of chemical reactions, including organic reactions, nanoalloy-growth, cellular processes and so on.<sup>8-11</sup> However, investigations for the degradation process of pesticides, which can help understanding and defining their

degradation mechanisms, are not involved up to now.

It is known that the long-term indiscriminate use of pesticides has led to the accumulation of them and brought about serious problems in food and environment.<sup>12</sup> In fact, less than 0.3% of the pesticides applied actually reaches their targeted pests,<sup>13</sup> and thus about 99.7% of the remaining forms are harmful to the non-target organisms and causes secondary pollution after degradation. There have been various stakeholders to reduce or eliminate the use of pesticides, but the degradation mechanisms possessing crucial significance in decreasing their side effects remain unclear and challengeable.<sup>14,15</sup>

Monitoring the degradation process of pesticides by using iDFM technique to monitor the LSPR optical properties of AgNPs was a feasible alternative, since iDFM technique takes advantages of high efficiency, less time consuming and high signal-to-noise ratio by investigating the shape, size, composition and surrounding medium of nanoparticles.<sup>16-18</sup> Although there are many researches using AgNPs as a chemical probe,<sup>19-21</sup> the application of iDFM technique to monitor the degradation process of pesticides through observation of the dynamic changes in LSPR scattered light of single AgNPs has not been developed up to now.

Sodium dimethyldithiocarbamate (NaDDC), a common pesticide,<sup>22</sup> is also a kind of dithiocarbamate acids (DTC). Most of the investigations about the decomposition mechanisms of NaDDC are conducted through measuring the amount of CS<sub>2</sub> under acidic condition,<sup>23-25</sup> but the decomposition mechanisms of NaDDC in neutral and basic conditions have been neglected for a long time due to the fact that the dialkyl DTC are very stable in these conditions.<sup>26</sup>

<sup>a</sup> Key Laboratory of Luminescent and Real-Time Analytical Chemistry (Southwest University), Ministry of Education, College of Pharmaceutical Sciences, Southwest University, Chongqing 400716, P. R. China. Fax: +86 23 68367257; Tel: +86 23 68254059. E-mail: liuhui78@swu.edu.cn

<sup>b</sup> Chongqing Key Laboratory of Biomedical Analysis (Southwest University), Chongqing Science & Technology Commission, College of Chemistry and Chemical Engineering, Southwest University, Chongqing 400715, China. Fax: +86 23 68367257; Tel: +86 23 68254659. E-mail: chengzhi@swu.edu.cn

† Electronic Supplementary Information (ESI) available: [additional DFM images (Fig.S1-S9) and the typical dynamic iDFM of monitoring (Movie S1-S2)]. See DOI: 10.1039/b000000x/

It was reported that after reacting with the corresponding chlorides, the product of NaDDC can degrade into  $\text{RSNa}$ ,  $\text{Na}_2\text{S}$ ,  $\text{Na}_2\text{CO}_3$  and  $\text{NH}(\text{CH}_3)_2$ , when heated under reflux for five hours with five moles of aqueous alcoholic alkali.<sup>27</sup> Nonetheless, the mechanisms of the basic decomposition of NaDDC are not clear until now. Therefore, NaDDC was selected as an example to investigate the degradation process of pesticides in this study.

Establishing a highly sensitive dynamic detection method and quantitatively real-time monitoring the decomposition process of NaDDC is of great environmental significance as well. NaDDC has various applications in agriculture, industry and medicine.<sup>22</sup> If uptaken by the plants, NaDDC would transformed into other fungitoxic compounds to achieve therapeutic effect.<sup>28</sup> For its excellent ability of chelation with metal ions, NaDDC has also been commercially used in metal finishing operations and treatment of wastewater by forming the metal precipitation.<sup>29, 30</sup> However, the disadvantages of NaDDC use, such as uncontrollability of dosage, relatively high cost, and difficulty in detecting the residual have been found.<sup>31</sup> Mover, NaDDC is considered as an important precursor of NDMA, a suspected carcinogen,<sup>32, 33</sup> and will produce toxic  $\text{CS}_2$  after acidic decomposition.<sup>25</sup> Conventional techniques employed in the detection of NaDDC, such as UV absorption spectra,<sup>34</sup> high-performance liquid chromatography (HPLC),<sup>35</sup> and capillary electrophoresis,<sup>36</sup> suffer problems of high detection limits, complicated operations and inferior efficiency. In contrast, single nanoparticle analysis technique can be used as a new dominant platform for the detection of NaDDC or other pesticides.

By using iDFM at single nanoparticle level to quantitatively resolve the dynamic process in terms of mechanisms understanding of the reaction,<sup>37</sup> herein we monitor the decomposition reaction of NaDDC in both neutral and basic conditions on the basis of the reaction between the  $\text{S}^{2-}$  which released from the degradation process and AgNPs which acts as a nanoprobe for it can result in decreasing LSPR light scattering signals.

## EXPERIMENTAL SECTION

### Materials

Sodium citrate ( $\text{Na}_3\text{C}_6\text{H}_5\text{O}_7 \cdot 2\text{H}_2\text{O}$  AR, 99.0%) and copper sulfate ( $\text{CuSO}_4 \cdot 5\text{H}_2\text{O}$  AR, 99.0%) were obtained from Tianjin Regent Chemicals Co. Ltd.. Silver nitrate ( $\text{AgNO}_3$  AR, 99.8%) was purchased from Shanghai Shenbo Chemical Engineering Co. Ltd.. Glycerin was obtained from Chongqing Chuandong Chemical (Group) Co. Ltd.. Zinc sulfate ( $\text{ZnSO}_4$  AR, 99.5%) was purchased from Hunan Xiangzhong Geological Experiment Research Institute. Sodium Dimethyldithiocarbamate ( $\text{C}_3\text{H}_6\text{NNaS}_2 \cdot 2\text{H}_2\text{O}$  AR, 98.0%) was acquired from Beijing J & K Technology Co. Ltd.. Other chemicals were analytical reagent grade and were used without further treatment. Milli-Q purified water ( $18.2 \text{ M}\Omega$  at  $25^\circ\text{C}$ ) was used throughout.

### Apparatus

Scattered light iDFM technique was carried out through a BX51 optical microscope (Olympus, Japan) equipped with a high numerical dark-field condenser (U-DCW, 1.2–1.4). The scattered light was collected by a  $100\times$  objective lens and the images were

taken by a DP72 single chip true color CCD camera (Olympus, Japan). The images were analyzed with Image-Pro Plus 6.0 (IPP) software (Media Cybernetics, USA). The size and morphology of the AgNPs were imaged by a Hitachi S-4800 scanning electron microscopy (SEM, Tokyo, Japan). The UV-vis absorption spectroscopy of NaDDC was performed with a UV-3600 spectrophotometer (Hitachi, Tokyo, Japan). A vortex mixer (QL-901, Kylin-Bell, Haimen, China) was used to blend the solutions. A centrifuge (H1650-W, Xiangyi, Hunan, China) was employed to separate the precipitates and supernatants.

### Preparation of AgNPs

AgNPs were prepared using previously reported methods. Firstly, a 50 mL glycerol/water mixture (20 vol% glycerol) was stirred (1200 rpm, 2.5 cm stirring bar) in a 100 mL flask and heated up to  $95^\circ\text{C}$ . Then, 9 mg silver nitrate was added to the solution, and 1 min later, 1 mL sodium citrate (3%) was added into the mixture again. The reaction mixture was stirred for 1 h at  $95^\circ\text{C}$ . The color change rate of the solution was found to be slightly slower than that of the classical Lee and Meisel method.<sup>38</sup> After the reaction completed, the colloid was stored at  $4^\circ\text{C}$ .

### Scattered light iDFM of AgNPs

To observe the scattered light changes of AgNPs either in intensity or color during its reaction with NaDDC, a homemade device with of a slide glass and cover glass was used to produce a simulated flow cell.<sup>8</sup> Scattered light iDFM of AgNPs deposited at the bottom of the cell were taken and an area containing AgNPs was selected for real-time monitoring. The NaDDC solution was added into the cell to initiate the degradation in neutral and alkaline conditions, respectively. The phosphate buffer (PB) was used to create an alkaline environment of pH 9.0. Then, the scattered light iDFM of the same area were obtained at different time points.

### The inhibition of metal ions on the degradation of NaDDC

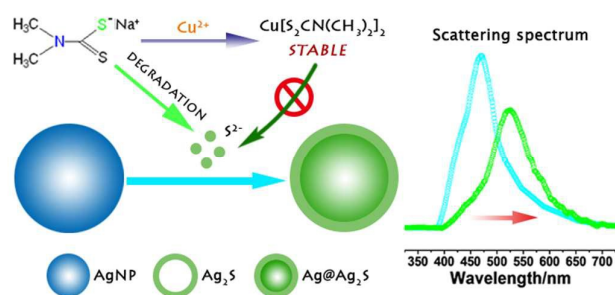
Like most pesticides, NaDDC would produce toxic substances after degradation. Besides decreasing the usage amount, inhibiting its degradation in the environment was also a way to reduce the environmental hazards of NaDDC. As mentioned before, metal ions could form complex with NaDDC, thus inhibiting its degradation, so we involved this facet of the research later. Herein  $\text{Cu}^{2+}$  and  $\text{Zn}^{2+}$  ions were chosen for the inhibition experiment. Particularly, the inhibition of  $\text{Cu}^{2+}$  on the degradation of NaDDC was made in neutral and alkaline conditions because the complex of  $\text{Cu}^{2+}$  and NaDDC was most stable.

### Data analysis

The statistics of light intensity and the red, green and blue (RGB) color proportion of the scattered light of AgNPs at single nanoparticle level were carried out using Image-Pro Plus (IPP) 6.0 software.<sup>16</sup>

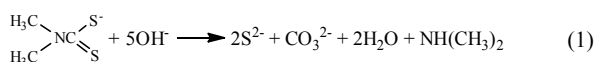
## RESULTS AND DISCUSSIONS

### Principle of the real-time imaging of the dynamic degradation of NaDDC.

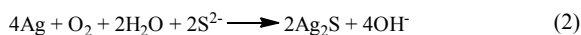


**Scheme 1.** Schematic illustration of real-time monitoring of the degradation process of NaDDC by using the LSPR scattering light of AgNPs and the inhibition of metal ions such as Cu (II) ions.

When decomposition of NaDDC occurred,  $S^{2-}$  might be released according to references:<sup>27</sup>



Nevertheless, the reaction is very difficult to happen at room temperature. In such case, the presence of Ag in neutral and alkaline conditions makes the chemical equilibrium of equation 1 constantly shift to right since the generated  $S^{2-}$  can form  $Ag_2S$  with it:<sup>39-41</sup>



which supplies the monitoring with an exciting way. That is to say, single AgNPs can act as a good nanoprobe to monitor the decomposition reaction of NaDDC in neutral and basic conditions (Scheme 1) since the LSPR optical properties of silver nanoparticles (AgNPs) are sensitive to their surrounding environments,<sup>42, 43</sup> and the changes in scattering intensity and color of AgNPs could be observed and be used as the detecting signals.<sup>44, 45</sup>

### Interaction between AgNPs and NaDDC

The as-prepared AgNPs had an average size of  $47.69 \pm 6.65$  nm, with a very narrow dispersion (Fig. 1A), displaying a yellow LSPR absorption band characteristic at 409.5 nm and blue scattering characteristic at 442 nm (Fig. 1B). The scattered blue light of the AgNPs ensemble in the solution was identical to those deposited on the glass slide under a white light source (Fig. S1†). Owing to the nonuniformity of AgNPs, there were some nanoparticles scattering other colors,<sup>46</sup> but we only considered the blue spherical particles.

The LSPR features either absorption or scattering are sensitive to the environments.<sup>47, 48</sup> Fig. 2A-F showed that the time-dependent

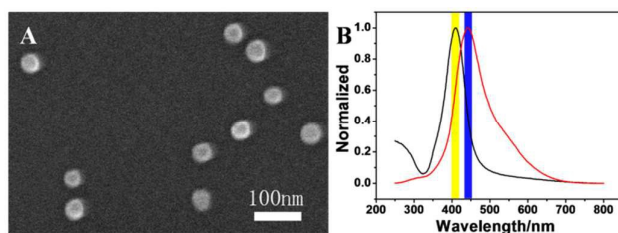


**Fig. 1** The characterization of the synthetic AgNPs: (A) SEM images and (B) UV absorption (black) and LSPR scattering (red) spectra.

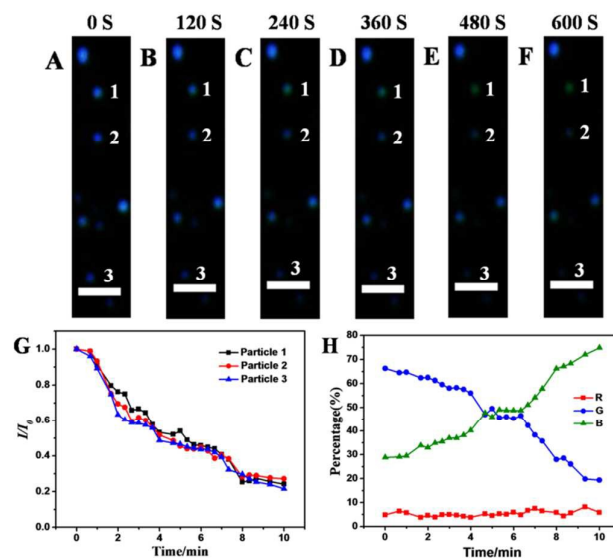


**Fig. 2** Scattered light iDFM of AgNPs during its reaction with NaDDC: (A-F) time-dependent images captured at different time points, with a latency time of 120s;  $C_3H_7NNaS_2$ ,  $1.0 \times 10^{-3}$  mol  $L^{-1}$ ; pH, 7; (G) time-dependent intensity analysis of the corresponding particles in (A-F); (H) time-dependent RGB analysis of the color-changed Particle 1 in (A-F). The scale bar is 2  $\mu m$  for all images.

evolution process of the scattered light iDFM for these AgNPs with the addition of 1 mM NaDDC aqueous solution. The blue scattering light of the AgNPs gradually declined with the addition of NaDDC, and some of the scattering light changed from blue to green (Particles 1 in Fig. 2A-F). This process remains about 10 min, and most of the blue spots disappeared. It should be noted that there were still some blue AgNPs on the glass (Particle 2 and 3) in which slight changes have occurred, displaying that the evolution process of different AgNPs are particle dependent in terms of the shape, the size and surficial state. The light intensity of three typical particles and the RGB proportion of the color-changed particle were analyzed to quantify the scattering light of AgNPs. As shown in Fig. 2G, the light intensity of Particles 1-3 gradually decreased to lower than 30% of their original light intensity. Moreover, the change of RGB proportion of Particle 1 which turned green after reaction was identical to the color changes that were observed by imaging (Fig. 2H). With the increase of reaction time, percentage of blue (PB) gradually decreased from 66% to 19%, while percentage of green (PG) gradually increased from 29% to 75%. Percentage of red (PR) was always maintained at 4-8% during the whole degradation process of NaDDC.

The evolution process of the scattered light iDFM for these AgNPs with the addition of NaDDC discloses the reaction features. The HRTEM images (Fig. 3A and B) showed that a very thin layer of  $Ag_2S$  has really formed on the surface of the AgNPs. The EDS analysis (Fig. 3C) evidenced the content of S was about 2%. Although the content was ultralow, it could lead to obvious variation in dark-field imaging.<sup>45</sup> That is to say,  $Ag_2S$  layer has been really

formed, reflecting the release of  $S^{2-}$  in both in neutral and alkaline conditions, which is the main driving force of degradation reaction

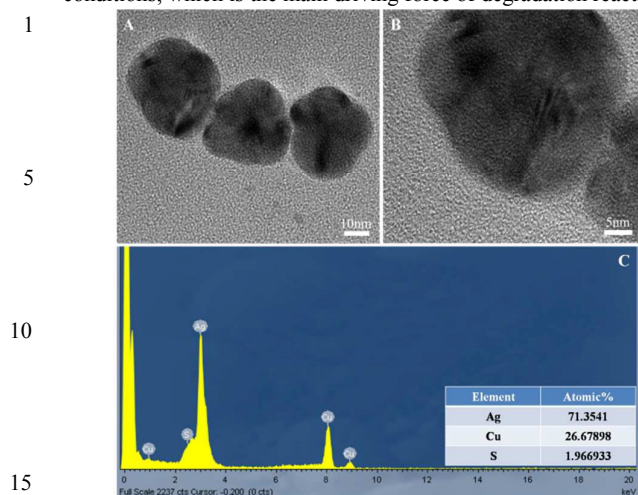


**Fig. 3** The characterizations of AgNPs after exposure to NaDDC aqueous solution for 10 min: (A) HRTEM image of AgNPs, (B) further magnified HRTEM image and (C) EDS spectrum of AgNPs after the completion with NaDDC.

of NaDDC, and makes chemical equilibrium shift to the right continuously.

#### Concentration-dependent degradation of NaDDC in both neutral and alkaline conditions

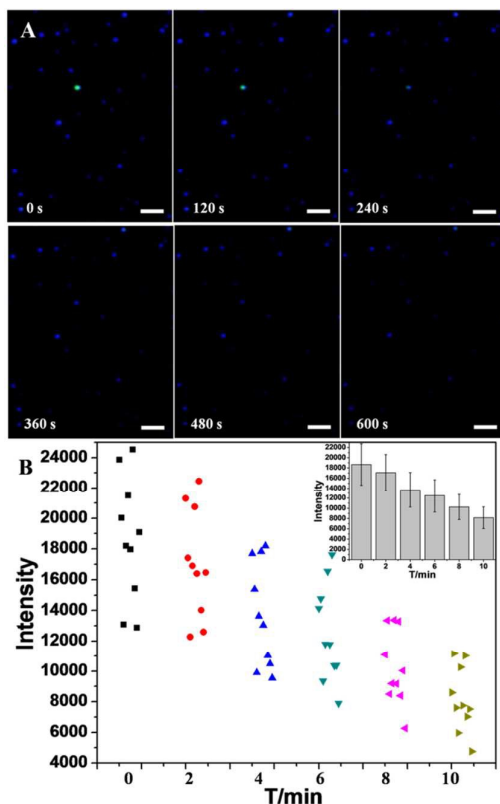


**Fig. 4** Scattered light iDFM of AgNPs after the 0.5 mM NaDDC aqueous solution added into the cell (A) and the scattering intensity statistics of the chosen 10 AgNPs over time

(B). The insert showed the changes in the total intensity of AgNPs. The scale bar corresponds to 2  $\mu\text{m}$  for all images.

In order to identify that the release of  $S^{2-}$  resulted from the reaction in neutral and alkaline conditions, both 0.5 mM and 1.0 mM of NaDDC were tested. This reaction was NaDDC-concentration dependent. Compared with 1 mM NaDDC solution (Fig. 2), with the addition of 0.5 mM NaDDC aqueous solution, the reaction progress proceeded much milder, and no color change, but the scattering intensity of AgNPs declined over time (Fig. 4A). Fig. 4B showed the scattering intensity statistics of the chosen 10 AgNPs in 0, 2, 4, 6, 8, 10 time point, which intuitively indicated the change trends of scattering intensity. The whole degradation process became longer as well in this concentration, and it ended after about 20 minutes. The scattering light intensity of AgNPs in Fig. 5D did not change any more, showing the termination of reaction.

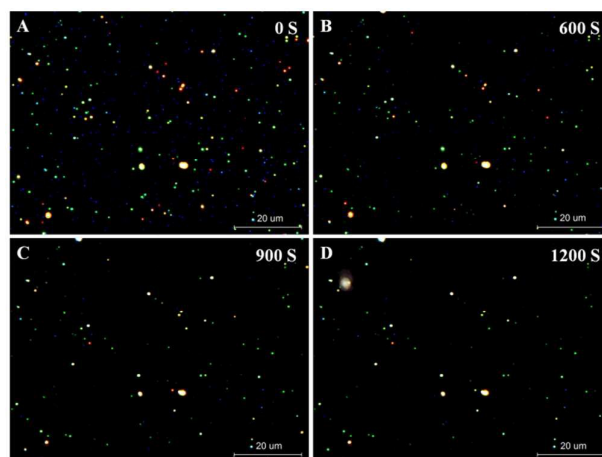


**Fig. 5** Light scattering iDFMs of AgNPs of the same area after the addition of 0.5 mM NaDDC aqueous solution at 0 s, 600 s, 900 s and 1200 s.

0.5 mM NaDDC alkaline solution was applied to show the differences compared to neutral condition (Fig. 6). The reaction was more intense and unlike the neutral solution, 0.5 mM NaDDC alkaline solution could make the scattering light color of some AgNPs gradually change from blue to green, with a more obvious decline in light intensity.

If increasing the concentration of NaDDC alkaline solution to 1 mM, its reaction with AgNPs was too intense that the overall

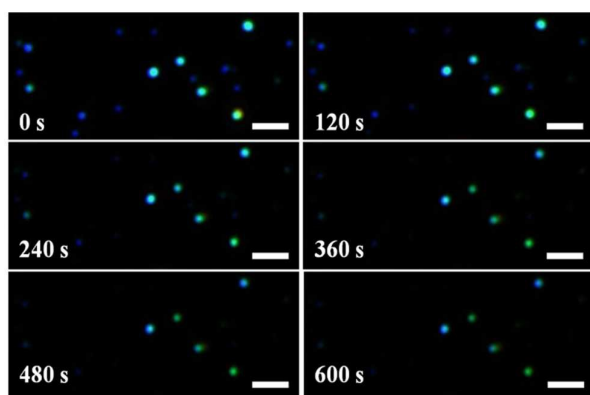


Fig. 6 Light scattering iDFMs of AgNPs after the 0.5 mM NaDDC alkaline solution (pH, 9) added into the cell. The scale bar is 2  $\mu$ m for all images.

1 morphology of AgNPs in the bottom changed a lot (Fig. S2 $\dagger$ ), and  
 2 most of them disappeared after reaction. That is to say, NaDDC  
 3 could produce more S<sup>2-</sup> after degradation in alkaline condition and  
 4 when the concentration of NaDDC reached a certain value, it could  
 5 change the scattering light color of AgNPs. DFM images before and  
 6 after reaction at pH 7 and 9 were captured to show the difference in  
 7 neutral and alkaline conditions (Fig. S3 $\dagger$ ).

8 The scattering light color change of the AgNPs should be ascribed  
 9 to the wavelength shifts with the reaction process (Fig. 7). The  
 10 scattering spectrum of the same AgNP before and after reaction with  
 11 1 mM NaDDC was also measured and it underwent a redshift from  
 12 471 nm to 526 nm (Fig. 7A). When 0.5mM NaDDC aqueous  
 13 solution was employed, the reaction became milder and the  
 14 scattering light had little color change, with a spectral redshift about  
 15 27.5 nm (Fig. 7B). When 0.5mM NaDDC alkaline solution was  
 16 employed, the scattering light color of AgNPs underwent a color  
 17 change, and the spectrum shifted from 447 nm to 497.5 nm (Fig. 7C).  
 18 The more redshift of the scattering light of AgNPs in alkaline  
 19 condition indicated that there were more Ag<sub>2</sub>S generated on the  
 20 surface of AgNP compared to neutral condition. Namely, NaDDC  
 21 could decompose more intensively and produce more S<sup>2-</sup> in alkaline  
 22 condition, which supported our deduction considering that OH<sup>-</sup> was  
 23 the major reactant in the decomposition reaction of NaDDC.

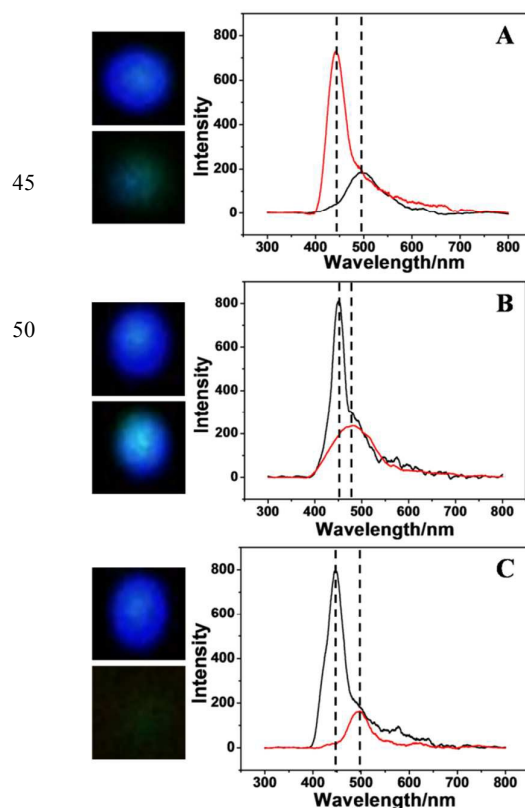
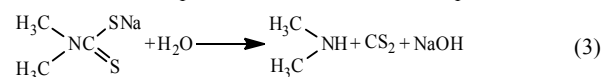


Fig. 7 The scattering spectral changes of AgNPs before and after the 1 mM aqueous (A), 0.5 mM aqueous (B) and 0.5 mM alkaline (C) NaDDC solution added into the cell, respectively. The dark field microscopic images and corresponding resonant scattering spectra of the chosen Ag nanoparticles before (black curves) and after (red curves) their exposure to NaDDC solution for 10 min.

### Real-time monitoring of the degradation of NaDDC

24 Then the *in situ* degradation of NaDDC was real-time monitored. Its  
 25 degradation in acid condition has been researched, and the  
 26 mechanisms of decomposition can be described as equation 3:<sup>24</sup>

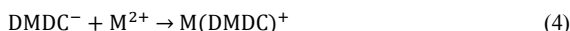


27 Thus the acid decomposition was not involved. Here we  
 28 considered reactions at pH 7 and pH 9. With the addition of 1 mM  
 29 NaDDC aqueous solution at pH 7, the scattering light color of  
 30 AgNPs gradually changed from blue to green, with an obvious  
 31 decline in light intensity, even if the scattering light of some AgNPs  
 32 disappeared (Movie. 1 $\dagger$ ). In contrast, with the addition of 1 mM  
 33 NaDDC PB solution at pH 9, the reaction became more intense and  
 34 the scattering light color of AgNPs changed from blue to green more  
 35 quickly, most of them disappeared after the reaction (Movie. 2 $\dagger$ ).  
 Other concentrations were used to try and the 10  $\mu$ M NaDDC  
 aqueous solution was the lowest concentration which could cause the  
 scattering light intensity change of AgNPs (Fig. S4 $\dagger$ ).

### The complexation between NaDDC and metal ions

Metal ions, for example the copper (II) ions, could generate a 2:1  
 complex with NaDDC, thus inhibiting its degradation. The resulting

complex was very stable and would not produce any toxic substances. NaDDC had also been commercially used as metal-chelator for this reason. The following reactions between metals and dimethyldithiocarbamate (DMDC) occur in equation 4 and 5 as:<sup>49</sup>



However, the dosage of NaDDC was difficult to control in the chelation. The application of DFM could resolve this problem. If NaDDC was overfeeding, the remaining NaDDC in solution could continue to change the scattering light of AgNPs after chelation, which could be intuitively observed by DFM.

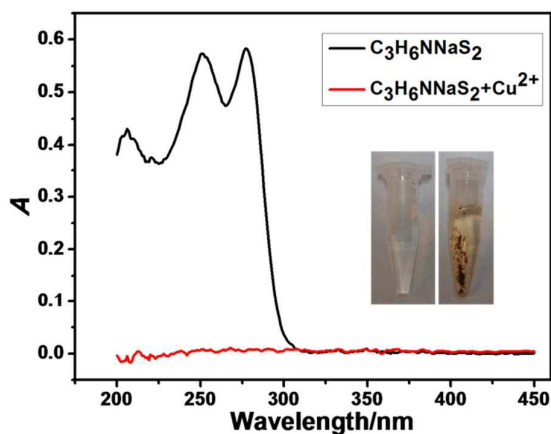


**Fig. 8** The UV absorption spectrum of NaDDC solution before and after the addition of  $\text{CuSO}_4$ . The insert showed the photographs of NaDDC solution with (right) or without (left) the addition of half the amount of  $\text{CuSO}_4$ .

Considering that the complex of  $\text{Cu}^{2+}$  and NaDDC was the most stable,<sup>50</sup> copper (II) ions were selected for experiment. When 0.5 mM  $\text{CuSO}_4$  solution was added to the 1 mM NaDDC solution, there were many brown precipitates produced (Fig. S5†). After centrifugation, the supernatant was taken for UV absorption measurement (Fig. 8). The absorption peaks at 251 nm and 277 nm disappeared, indicating the NaDDC in solution was removed. The UV absorption spectrums before and after complexation in neutral, acid and alkaline conditions were presented in Fig. S6† respectively, and the results showed the complexation between  $\text{Cu}^{2+}$  and NaDDC could happen irrespective pH.

Then we added the supernatant into the simulated flow cell for dark-field imaging, to see if it could make changes on the scattering of AgNPs. As shown in the DFM images in Fig. 9A, the scattering light of AgNPs did not change. The intensity statistics by IPP (Fig. 9B) also supported this consequence. The complexation of  $\text{Zn}^{2+}$  and NaDDC was also investigated (Fig. S7†), and the results showed  $\text{Zn}^{2+}$  could inhibit the decomposition of NaDDC.

To investigate the stoichiometric ratio between NaDDC and  $\text{Cu}^{2+}$ , three sets of solution (The ratio of the amount of NaDDC and  $\text{Cu}^{2+}$

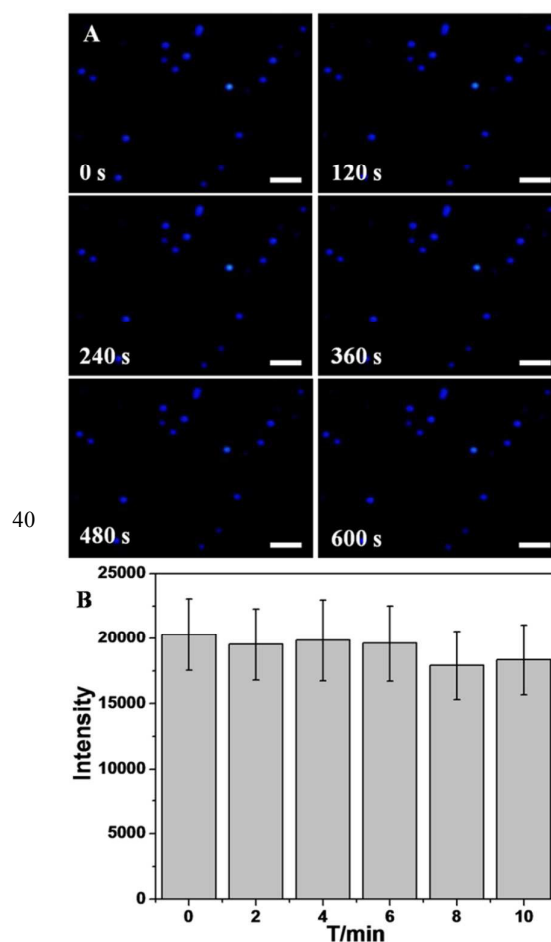


**Fig. 9** Scattered light iDFM of AgNPs after the supernatant (NaDDC: $\text{Cu}^{2+}$  = 2:1) added into the cell (A). The scattering intensity of the chosen AgNPs remained the same before and after the reaction, accompanied with a small mechanical error (B). The scale bar corresponds to 2  $\mu\text{m}$  for all images.

was 4:1, 2:1 and 1:1 respectively) were prepared, in which 1 mM NaDDC aqueous solution and 0.25 mM, 0.5 mM, 1 mM  $\text{CuSO}_4$  aqueous solution were employed correspondingly. Upon mixed, they reacted and produced many brown precipitates. Removing the precipitates by centrifugation and drawing the supernatant into the flow cell, the dynamic images of the reaction were taken by DFM. The supernatant of the first group (NaDDC: $\text{Cu}^{2+}$  = 4:1) could still change the scattering light intensity of AgNPs, showing  $\text{Cu}^{2+}$  could not inhibit the hydrolysis of NaDDC thoroughly in this ratio (Fig. S8†), and thus proving the feasibility of applying DFM to estimate whether NaDDC was excessive when used in metal removal.

The supernatant of the second group could not change the scattering light of AgNPs, showing in this ratio  $\text{Cu}^{2+}$  and NaDDC completely complexed (Fig. 9). The result was the same with former when excess  $\text{Cu}^{2+}$  ions (the third group) were employed to inhibit the hydrolysis of NaDDC (Fig. S9†). The stoichiometric ratio between NaDDC and  $\text{Cu}^{2+}$  was 2:1. The inhibition of  $\text{Cu}^{2+}$  in alkaline condition was also investigated (Fig. S10†), and the result showed  $\text{Cu}^{2+}$  could inhibit the hydrolysis of NaDDC in this condition. The stability of the complex of  $\text{Cu}^{2+}$  and NaDDC was also investigated

by adding the reaction solution into the flow cell without centrifugation, and the results showed that the complex was stable and could not induce the change of the scattering light of AgNPs (Fig. S11†).

## Conclusions

In summary, we achieved a real-time monitoring of the dynamic degradation process of NaDDC by DFM and deduced the chemical formulas of the degradation, expanding SNA technique to a new field. As far as we know, it is also for the first time to research the degradation dynamics of NaDDC in neutral and alkaline conditions. The reaction between NaDDC and AgNPs didn't have specific regulation, but through RGB analysis and scanning spectrum before and after reaction we developed a semi-quantitative detection method of NaDDC. The minimum response concentration was 10  $\mu$ M, lower than the conventional methods. The pesticide could change the intensity as well as the color of AgNPs, making the process of degradation visual and easy to analyze. Besides NaDDC, our method could also be utilized to monitor the decomposition reactions of other pesticides. The HRTEM images were taken to prove the formation of Ag<sub>2</sub>S on the surface of the AgNPs. The whole decomposition process of NaDDC was monitored in nanoscale.

The other work was to study whether the metal ions could inhibit the neutral- and alkaline-hydrolysis of NaDDC. The result showed they could and the ratio of NaDDC and Cu<sup>2+</sup> ions was 2:1, so we could declare that the inhibition of metal ions on the degradation of NaDDC was irrespective of pH. Our strategy visualized the NaDDC present in solution and added benefits to resolving the problem of overfeeding in NaDDC use. These conclusions could help understanding and defining this kind of degradation mechanisms and contribute to reducing or eliminating the hazards of NaDDC.

## Acknowledgements

This work was financially supported by the National Natural Science Foundation of China (NSFC, No. 21535006).

## Notes and references

<sup>a</sup> Key Laboratory of Luminescent and Real-Time Analytical Chemistry (Southwest University), Ministry of Education, College of Pharmaceutical Sciences, Southwest University, Chongqing 400716, P. R. China.

<sup>b</sup>Chongqing Key Laboratory of Biomedical Analysis (Southwest University), Chongqing Science & Technology Commission, College of Chemistry and Chemical Engineering, Southwest University, Chongqing 400715, China

† Electronic Supplementary Information (ESI) available: [additional DFM images (Fig.S1-S9) and the typical dynamic iDFM of monitoring (Movie S1-S2).]. See DOI: 10.1039/b000000x/

1. A. J. Haes, L. Chang, W. L. Klein and R. P. Van Duyne, *J. Am. Chem. Soc.*, 2005, **127**, 2264-2271.

2. Y. Choi, Y. Park, T. Kang and L. P. Lee, *Nat. Nanotechnol.*, 2009, **4**, 742-746.

3. X.-L. Hu, H.-Y. Jin, X.-P. He, T. D. James, G.-R. Chen and Y.-T. Long, *ACS Appl. Mater. Interfaces*, 2015, **7**, 1874-1878.

4. Z. Chen, J. Li, X. Chen, J. Cao, J. Zhang, Q. Min and J.-J. Zhu, *J. Am. Chem. Soc.*, 2015, **137**, 1903-1908.

5. L. Zhang, Y. Li, D.-W. Li, C. Jing, X. Chen, M. Lv, Q. Huang, Y.-T. Long and I. Willner, *Angew. Chem. Int. Edit.*, 2011, **50**, 6789-6792.

6. L. P. Wu, Y. F. Li, C. Z. Huang, Q. Zhang, *Anal. Chem.*, 2006, **78**, 5570-5577.

7. C. Z. Huang, K. A. Li, S. Y. Tong, *Anal. Chem.*, 1996, **68**, 2259-2263.

8. Y. Liu and C. Z. Huang, *ACS Nano*, 2013, **7**, 11026-11034.

9. L. Shi, C. Jing, W. Ma, D.-W. Li, J. E. Halls, F. Marken and Y.-T. Long, *Angew. Chem. Int. Edit.*, 2013, **52**, 6011-6014.

10. H. Yang, Y. Liu, P. F. Gao, J. Wang and C. Z. Huang, *Analyst*, 2014, **40139**, 2783-2787.

11. T. Xie, C. Jing, W. Ma, Z. Ding, A. J. Gross and Y.-T. Long, *Nanoscale*, 2015, **7**, 511-517.

12. S. Singh, R. Gupta and S. Sharma, *J. Hazard. Mater.*, 2015, **291**, 102-110.

13. D. Pimentel and M. Burgess, *Environ. Dev. Sustainabil.*, 2012, **14**, 1-2.

14. S. B. Emery, A. Hart, C. Butler-Ellis, M. G. Gerritsen-Ebben, K. Machera, P. Spanoghe and L. J. Frewer, *Hum. Ecol. Risk Assess.*, 2014, **21**, 1062-1080.

15. Y. Zhan and M. H. Zhang, *Sci. Total Environ.*, 2014, **472**, 517-529.

16. Y. Liu and C. Z. Huang, *Chem. commun.*, 2013, **49**, 8262-8264.

17. W.-G. Qu, B. Deng, S.-L. Zhong, H.-Y. Shi, S.-S. Wang and A.-W. Xu, *Chem. commun.*, 2011, **47**, 1237-1239.

18. S. Berciaud, L. Cognet, P. Tamarat and B. Lounis, *Nano letters*, 2005, **5**, 515-518.

19. A. D. McFarland and R. P. Van Duyne, *Nano letters*, 2003, **3**, 1057-1062.

20. Y. Luo, S. Shen, J. Luo, X. Wang and R. Sun, *Nanoscale*, 2015, **7**, 690-700.

21. V. Tharmaraj and J. Yang, *Analyst*, 2014, **139**, 6304-6309.

22. J. M. Goldman, A. S. Murr, A. R. Buckalew and R. L. Cooper, *Toxicol. Sci.*, 2008, **104**, 107-112.

23. K. I. Aspila, V. S. Sastri and C. L. Chakrabarti, *Talanta*, 1969, **16**, 1099-1102.

24. L. E. Lopatecki and W. Newton, *Can. J. Bot.*, 1952, **30**, 131-138.

25. E. Humeres, N. A. Debacher, M. M. d. S. Sierra, J. D. Franco and A. Schutz, *J. Org. Chem.*, 1998, **63**, 1598-1603.
26. S. J. Joris, K. I. Aspila and C. L. Chakrabarti, *Anal. Chem.*, 1970, **42**, 647-651.
27. M. Kulka, *Can. J. Chem.*, 1956, **34**, 1093-1100.
28. H. M. Dekhuijzen, *Nature*, 1961, **191**, 198-199.
29. M. M. Matlock, K. R. Henke and D. A. Atwood, *J. Hazard. Mater.*, 2002, **92**, 129-142.
30. M. J. McFarland, C. Glarborg and M. A. Ross, *Water. Environ. Res.*, 2012, **84**, 2086-2089.
31. C. A. Erven, *Met. Finish.*, 2001, **99**, 8-19.
32. W. A. Mitch and D. L. Sedlak, *Environ. Sci. Technol.*, 2004, **38**, 1445-1454.
33. C. Lee, W. Choi, Y. G. Kim and J. Yoon, *Environ. Sci. Technol.*, 2005, **39**, 2101-2106.
34. T. Yamase, H. Kokado and E. Inoue, *B. Chem. Soc. Jpn.*, 1970, **43**, 934-935.
35. X. Z. Cao and Y. M. Li, *Anal. Methods*, 2012, **4**, 2996-3001.
36. A. J. Nitowski, A. A. Nitowski, J. A. Lent, D. W. Bairley and D. Van Valkenburg, *J. Chromatogr. A*, 1997, **781**, 541-545.
37. J. G. Smith, Q. Yang and P. K. Jain, *Angew. Chem. Int. Edit.*, 2014, **53**, 2867-2872.
38. D. Steinigeweg and S. Schlucker, *Chem. commun.*, 2012, **48**, 8682-8684.
39. S. Lilienfeld and C. E. White, *J. Am. Chem. Soc.*, 1930, **52**, 885-892.
40. J. Zeng, J. Tao, D. Su, Y. Zhu, D. Qin and Y. N. Xia, *Nano letters*, 2011, **11**, 3010-3015.
41. C. H. Fang, Y. H. Lee, L. Shao, R. B. Jiang, J. F. Wang and Q.-H. Xu, *ACS Nano*, 2013, **7**, 9354-9365.
42. Y. Liu and C. Z. Huang, *Nanoscale*, 2013, **5**, 7458-7466.
43. P. K. Jain, X. Huang, I. H. El-Sayed and M. A. El-Sayed, *Accounts Chem. Res.*, 2008, **41**, 1578-1586.
44. J. Hao, B. Xiong, X. Cheng, Y. He and E. S. Yeung, *Anal. Chem.*, 2014, **86**, 4663-4667.
45. B. Xiong, R. Zhou, J. Hao, Y. Jia, Y. He and E. S. Yeung, *Nat. Commun.*, 2013, **4**, 1708.
46. P. D. Nallathamby, T. Huang and X.-H. N. Xu, *Nanoscale*, 2010, **2**, 1715-1722.
47. C. Burda, X. Chen, R. Narayanan and M. A. El-Sayed, *Chem. Rev.*, 2005, **105**, 1025-1102.
48. I. Choi, H. D. Song, S. Lee, Y. I. Yang, T. Kang and J. Yi, *J. Am. Chem. Soc.*, 2012, **134**, 12083-12090.
49. K. W. Weissmahr and D. L. Sedlak, *Environ. Toxicol. Chem.*, 2000, **19**, 820-826.
50. M. Hallaway, *Biochim. Biophys. Acta*, 1959, **36**, 3.

1

1

5

5

10

10

15

15

20

20